A NEW SNOUTED TREEFROG OF THE GENUS SCINAX (ANURA, HYLIDAE) FROM THE WHITE-SAND FORESTS OF CENTRAL AMAZONIA

Authors: Ferrão, Miquéias, Moravec, Jiří, Ferreira, Anthony S., Moraes, Leandro J. C. L., and Hanken, James

Source: Breviora, 573(1) : 1-36

Published By: Museum of Comparative Zoology, Harvard University

URL: https://doi.org/10.3099/0006-9698-573.1.1

BREVIORA

Museum of Comparative Zoology

US ISSN 0006-9698

CAMBRIDGE, MASS. 3 FEBRUARY 2022 NUMBER 573

A NEW SNOUTED TREEFROG OF THE GENUS *SCINAX* (ANURA, HYLIDAE) FROM THE WHITE-SAND FORESTS OF CENTRAL AMAZONIA

MIQUÉIAS FERRÃO,[1,2] JIŘÍ MORAVEC,[3] ANTHONY S. FERREIRA,[4] LEANDRO J. C. L. MORAES,[2,5] AND JAMES HANKEN[1]

ABSTRACT. We describe through integrative taxonomy a new species of snouted treefrog of the genus *Scinax* from white-sand forests of the Rio Negro Sustainable Development Reserve in Central Amazonia, Brazil. The new species is phylogenetically related to other *Scinax* with striped eyes and pulsed advertisement calls. It differs from other Amazonian species mainly by having snout–vent length 21.6–25.4 mm ($n=11$) in adult males and 24.8–27.0 mm ($n=9$) in females, snout subacuminate in dorsal view, a dark brown lateral stripe on each flank (fading posteriorly), brown tadpoles with labial keratodont row formula 2(2)/3 and keratodont row P-2 longer than P-1 and P-3, and an advertisement call consisting of a single pulsed note with a call duration of 502–652 ms, 79–105 pulses/note and a dominant frequency of 3,811–4,543 Hz. The new species clusters within a major, well-supported phylogenetic clade grouping several candidate and recently described species as well as species previously included in the former *Scinax staufferi* species group (viz., *S. cruentomma, S. fuscomarginatus, S. staufferi,* and *S. wandae*). The phylogenetic relationships and structural pattern in the advertisement calls of these species highlight the need for a redefinition and reevaluation of the monophyly of the *S. staufferi* species group.

KEY WORDS: bioacoustics; integrative taxonomy; morphology; Rio Negro Sustainable Development Reserve; *Scinax staufferi* species group; tadpoles

[1] Museum of Comparative Zoology, Harvard University, 26 Oxford Street, Cambridge, Massachusetts 02138, U.S.A.; e-mail: miqueiasferrao@fas.harvard.edu

[2] Coordenação de Biodiversidade, Instituto Nacional de Pesquisas da Amazônia, Av. André Araújo 2936, Manaus, AM 69067-375, Brazil

[3] Department of Zoology, National Museum, Cirkusová 1740, Prague, Czech Republic

[4] Programa de Capacitação Institucional, Instituto Nacional de Pesquisas da Amazônia, Av. André Araújo 2936, Manaus, AM 69067-375, Brazil

[5] Programa de Pós-Graduação em Zoologia, Universidade de São Paulo, Instituto de Biociências, Rua do Matão 321, Travessa 14, São Paulo, SP 05508-900, Brazil

INTRODUCTION

Diversity and taxonomy of the Amazonian snouted treefrogs of the genus *Scinax* Wagler, 1830 have attracted the attention of biologists for decades (e.g., Duellman, 1972a; Fouquette and Delahoussaye, 1977; Duellman and Wiens, 1993; Faivovich, 2002; Fouquet et al., 2007; Ferrão et al., 2016; Acosta-Galvis, 2018; Lopes et al., 2020). Nevertheless, results of the most recent studies show that species richness of the

genus remains surprisingly underestimated (Vacher et al., 2020).

Analysis of the regional diversity of *Scinax* in central-to-southwestern Amazonia revealed the existence of at least seven molecularly and phenotypically distinct clades, each representing a candidate species (Ferrão et al., 2016). Later, three of these clades were described as new species (Ferrão et al., 2017, 2018a, b), including *S. strussmannae* Ferrão, Moravec, Kaefer, Fraga and Lima, 2018b which is closely related to *S. cruentomma* (Duellman, 1972b) and *S. wandae* (Pyburn and Fouquette, 1971). Two other candidate species related to the latter two species await formal description. In addition, a recent wide-scale DNA barcoding study documented seven additional candidate species related to *S. cruentomma* and *S. wandae* (Vacher et al., 2020). These findings indicate that taxonomic knowledge of this group of small-sized *Scinax* is still incomplete and that underexplored Amazonian regions harbor a very rich and mostly unknown anuran diversity.

White-sand ecosystems (hereafter, WSE) of Central Amazonia are a good example of poorly explored environments (Adeney et al., 2016). The WSE represent patchily distributed habitats with nutrient-poor sandy soils covered by grasslands, shrubs, or forests with low-stature canopies (Eiten, 1978). Usually, these habitats are embedded in dense forests with nutrient-rich soils (Eiten, 1978). Although WSE cover a small portion (approximately 5%) of the Amazon territory, the species assemblages occupying them are unique (Adeney et al., 2016; Costa et al., 2020). Rapid biological inventories of WSE have documented new species in various taxonomic groups (e.g., Vriesendorp et al., 2006; Cohn-Haft et al., 2013). More recently, several endemic or specialist WSE species have been reported for plants (Fine and Baraloto, 2016; Vicentini, 2016), insects (Lamarre et al., 2016), birds (Capurucho et al., 2013; Borges et al., 2016), snakes (Fraga et al., 2018) and frogs (Rojas-Zamora et al., 2015; Carvalho et al., 2018; Ferrão et al., 2019).

The largest regions of WSE lie in the Negro-Solimões interfluve—one of the most inaccessible and consequently unexplored parts of Brazilian Amazonia. Aiming to improve biological knowledge of WSE in the Negro-Solimões interfluve, the Brazilian Research Program on Biodiversity (PPBio - INPA) installed a long-term sampling module in the Rio Negro Sustainable Development Reserve (RDS Rio Negro), which crosses a heterogeneous landscape covered by a mosaic of dense forests and WSE patches. Recent herpetological surveys conducted along this sampling module by our research team resulted in the rediscovery of the WSE treefrog *Osteocephalus vilarsi* (Melin, 1941) (Ferrão et al., 2019), the recorded association of the gecko *Hemidactylus palaichthus* Kluge, 1969 with the bromeliad *Aechmea huebneri* (Ferreira et al., 2019), and the discovery of candidate species belonging to several anuran genera including *Scinax* (M. Ferrão and A. P. Lima, personal communication).

Herein, using an integrative taxonomy approach, we describe a new species of *Scinax* from these WSE patches which has morphological affinities to *S. cruentomma* and *S. wandae*.

MATERIALS AND METHODS

Sampling

Specimens of the new species were collected between June 2018 and April 2020 in the PPBio sampling module of the RDS Rio Negro (03°03′31″S, 60°45′42″W; 73 m a.s.l.), municipality of Novo Airão, state of Amazonas, Brazil (Fig. 1). Adults were euthanized with 2% benzocaine topical solution, fixed in 10% neutral-buffered formalin, and preserved in 70% ethanol. Tissue samples were collected

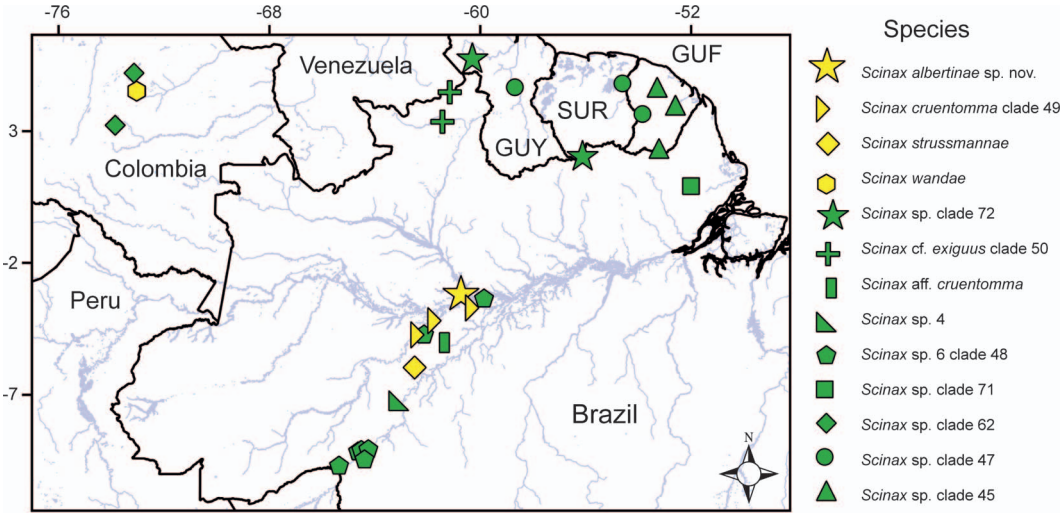

Figure 1. Geographic distribution of *Scinax albertinae* sp. nov. and closely related species with a red- or brown-striped iris based on samples included in our molecular analyses (Fig. 2). Country acronyms: GUF, French Guiana; GUY, Guyana; SUR, Suriname.

before fixation and stored in 100% ethanol. Seventeen tadpoles were euthanized with 2% benzocaine liquid solution (lot INPA-H 42855), while six others (lot INPA-H 42854) were reared in the laboratory until approximately stage 45 (Gosner, 1960). Both adults and tadpoles were deposited in the Amphibians and Reptiles Collection of the Instituto Nacional de Pesquisas da Amazônia, Manaus, Brazil (INPA-H).

Calls emitted by three adult males (INPA-H 42859, 42872, and an unvouchered individual) were recorded at the RDS Rio Negro sampling module at 1830 h on 25 April 2020. Calls were recorded with a Sennheiser K6/ME66 unidirectional microphone (Sennheiser, Germany) coupled to a Marantz PMD660 digital recorder (sampling rate 44.1 kHz, sample size 16 bits; Marantz, Japan). The microphone was positioned approximately 50 cm from each individual. Air temperature during recording was 25°C. Files were stored in WAV format and deposited in the Fonoteca Neotropical Jacques Vielliard (FNJV 50546–53) of the University of Campinas (UNICAMP), Campinas, Brazil.

Molecular phylogenetics

We extracted genomic DNA of four specimens of the new species by using a Wizard® Genomic DNA Purification Kit (Promega Corp., Madison, WI, USA) according to the manufacturer's protocol. A fragment of the 16S rRNA mitochondrial gene was amplified through polymerase chain reaction (PCR) using 16Sar and 16Sbr primers (Palumbi, 1991) and following protocols described in Ferrão et al. (2016). PCR products were purified using Exonuclease I and Thermosensitive Alkaline Phosphatase (Thermo Fisher Scientific, Waltham, MA, USA) and submitted to sequencing reactions using standard protocols of the Big Dye™ Terminator Kit (Applied Biosystems, Waltham, MA, USA). Amplicons were sequenced in an ABI 3730XL (Macrogen Inc., Seoul, Korea) using the forward primer. The software Bioedit (Hall, 1999) was used to edit the sequences, which ranged from 552 to 624 base pairs (bp). Newly generated sequences were deposited in the

online repository GenBank under accession numbers MW853693–MW853696.

To infer phylogenetic relationships of the new species, the above newly generated sequences were inserted into a data set containing homologous sequences retrieved from GenBank. These sequences represent 35 nominal and 16 candidate species of *Scinax,* covering all major species groups delimited in the taxonomic history of this genus (Faivovich, 2002; Faivovich et al., 2005). Nine other sequences of six species from the two most closely related genera *Ololygon* Fitzinger, 1843 and *Julianus* Duellman, Marion and Hedges, 2016 were included; a sequence of *Sphaenorhynchus surdus* (Cochran, 1953) was used as outgroup. Sequences retrieved from GenBank (Appendix 1) were published by Araujo-Vieira et al. (2019), Bell et al. (2012), Brusquetti et al. (2014), Faivovich et al. (2005), Ferrão et al. (2016), Fouquet et al. (2007), Frost et al. (2006), Guarnizo et al. (2015), Jansen et al. (2011), Lyra et al. (2017), Ron et al. (2018), Salducci et al. (2005), Vacher et al. (2020) and von May et al. (2019).

Sequences were aligned using the MAFFT online server with default parameters, except for the use of E-INS-i strategy (Katoh and Standley, 2013). The final matrix was composed of 146 terminals with 501 bp each. A comparison of Bayesian Information Criterion (BIC) values in a PartitionFinder (Lanfear et al., 2017) analysis indicated GTR + G + I as the most adjusted evolutionary model for this data set. Phylogenetic relationships were reconstructed using this model under Maximum Likelihood (ML) and Bayesian (BI) optimality criteria. The ML tree was inferred using IQTREE (Nguyen et al., 2015) as implemented in the webserver http://iqtree.cibiv.univie.ac.at (Trifinopoulos et al., 2016). Clade support was estimated with 10,000 ultrafast bootstrap replications (Hoang et al., 2018), 1,000 maximum iterations, and a minimum correlation coefficient of 0.99. The BI tree was inferred in MrBayes 3.2.6 (Ronquist et al., 2011) using four runs of 10 million generations with a Markov chain Monte Carlo algorithm. Each run had four Markov chains, with probabilities sampled every 1,000 generations. The BI analysis was implemented in the CIPRES online server https://www.phylo.org/. Stationarity of the posterior distributions and effective sample size (ESS >200) were examined in Tracer 1.7 (Rambaut et al., 2018) and the maximum clade credibility tree was extracted after discarding the first 25% of trees.

Pairwise genetic distances (uncorrected p-distance and Kimura-two-parameter distance; Kimura, 1980) between the new species and other *Scinax* species with a red- or brown-striped iris were calculated in MEGA 6 (Tamura et al., 2013). Intraspecific p-distances were also calculated for the new species and its closest relatives. Genetic distances were calculated using the method "pairwise deletion".

Morphology

Gender of adult specimens was determined according to presence (males) or absence (females) of vocal slits. Sixteen morphometric measurements were taken following Duellman (1970; horizontal eye diameter [ED], foot length [FL], head length [HL], head width [HW], internarial distance [IND], interorbital distance [IOD], snout–vent length [SVL], horizontal tympanum diameter [TD], tibia length [TL], and upper eyelid width [UEW]), Heyer et al. (1990; hand length [HAL], tarsus length [TAL], and thigh length [THL]), and Napoli (2005; eye–nostril distance [END], finger III disc diameter [3FD], and toe IV disc diameter [4TD]). These measurements were obtained to the nearest 0.1 mm using a digital caliper and an ocular micrometer coupled to a stereomicro-

scope. Snout shape terminology followed the definitions of Heyer et al. (1990). Webbing formulae followed Savage and Heyer (1967) as modified by Myers and Duellman (1982). Descriptions of coloration patterns in life were based on photographs and field notes. Descriptions of adult morphology are formatted as in Ferrão et al. (2018b).

Larval developmental stages of 17 tadpoles (lot INPA-H 42855) were determined according to the table of Gosner (1960) and ranged from stages 34 to 38. Morphological description was based on 10 tadpoles at stage 37. Eighteen morphometric measurements were taken following Altig and McDiarmid (1999; body length [BL], internarial distance [IND], interorbital distance [IOD], maximum tail height [MTH], tail length [TAL], tail muscle height at body–tail junction [TMH], tail muscle width at the same level as TMH [TMW], and total length [TTL]), Haas and Das (2011; body height [BH], maximum body width [BW], eye diameter [ED], eye–nostril distance [END], head width at the level of spiracle [HWLE], nostril–snout distance [NSD], oral disc width [ODW], distance of snout to center of spiracle [SS]), and Randrianiaina et al. (2011; ventral tube length [VTL] and spiracle length [STL]). Measurements were obtained to the nearest 0.1 mm with an ocular micrometer coupled to a stereomicroscope. Marginal papillae row (MPRL) and labial keratodont row (LKRF) formulae, as well as the formatting of tadpole description, followed Schulze et al. (2015). Descriptions of coloration patterns in life of tadpoles and metamorphs were based on specimens raised in the laboratory.

Vocalization

Two types of calls of an unvouchered and two vouchered (INPA-H 42859 and 42872) males were analyzed. The most commonly emitted vocalization was classified as advertisement, whereas the sporadic one was classified as territorial call because it was mainly emitted by spatially closest males and spatially distant males only sporadically emit this call type (*sensu* Toledo et al., 2015). The following 12 acoustic parameters were measured from advertisement calls: call duration (CD); intercall interval (ICI); call period (CP); call repetition rate (CR); number of pulses per call (PN); pulse duration (PD); interpulse interval (IPI); pulse period (PP); pulse rate (PRR); and low (LF), high (HF), and dominant frequency (DF). We also analyzed the second type of vocalization emitted by the same three males. The following parameters of territorial calls were measured: call duration (CDA); intercall interval (ICIA); call period (CPA); call rate (CRA); and low (LFA), high (HFA), and dominant (DFA) frequencies. Acoustic parameters were measured following the recommendations of Köhler et al. (2017).

Calls were analyzed using RAVEN 1.5 (Bioacoustics Research Program, 2014) configured as follows: Blackman window; 3 dB Filter Bandwidth, 80 Hz; overlap, 80%; hop size, 4.1 ms; and Discrete Fourier Transform size, 1,024 samples. Call repetition rate was calculated as 1 min divided by the call period, and pulse repetition rate as 1 sec divided by the pulse period. Dominant frequency was measured using the peak frequency function. Low and high frequencies were measured 20 dB below the peak frequency to avoid overlap with background noise. Call terminology follows Köhler et al. (2017) and advertisement call description follows Ferrão et al. (2018b). Graphic representations of calls were generated in the Program R environment (R Core Team, 2019) through the *seewave* package 2.0.5 (Sueur et al., 2008) using a Hanning window, 256 points of resolution (Fast Fourier Transform) and an overlap of 85%.

Interspecific comparisons

We compare the new species with all nominal species of *Scinax* distributed throughout Amazonia (Appendix 2): *S. baumgardneri* (Rivero, 1961); *S. blairi* (Fouquette and Pyburn, 1972); *S. boesemani* (Goin, 1966); *S. chiquitanus* (De la Riva, 1990); *S. cruentomma*; *S. danae* (Duellman, 1986); *S. exiguus* (Duellman, 1986); *S. funereus* (Cope, 1874); *S. fuscomarginatus* (Lutz, 1925a); *S. fuscovarius* (Lutz, 1925b); *S. garbei* (Miranda-Ribeiro, 1926); *S. ictericus* Duellman and Wiens, 1993; *S. iquitorum* Moravec, Tuanama, Pérez and Lehr, 2009; *S. jolyi* Lescure and Marty, 2000; *S. karenanneae* (Pyburn, 1993); *S. lindsayi* Pyburn, 1992; *S. madeirae* (Bokermann, 1964); *S. nebulosus* (Spix, 1824); *S. onca* Ferrão, Moravec, Fraga, Almeida, Kaefer and Lima, 2017; *S. oreites* Duellman and Wiens, 1993; *S. pedromedinae* (Henle, 1991); *S. proboscideus* (Brongersma, 1933); *S. rostratus* (Peters, 1863); *S. ruber* (Laurenti, 1768); *S. ruberoculatus* Ferrão, Fraga, Moravec, Kaefer and Lima, 2018a; *S. sateremawe* Sturaro and Peloso, 2014; *S. strussmannae* Ferrão, Moravec, Kaefer, Fraga and Lima, 2018b; *S. villasboasi* Brusquetti, Jansen, Barrio-Amorós, Segalla and Haddad, 2014; *S. wandae*; and *S. x-signatus* (Spix, 1824). Detailed comparisons are provided for closely related species as indicated by molecular phylogenetic relationships (*S. cruentomma, S. exiguus, S. wandae,* and *S. strussmannae*) and for species with similar morphology and advertisement calls (*S. baumgardneri, S. blairi, S. exiguus,* and *S. lindsayi*).

RESULTS

Phylogenetic relationships and genetic distances

Phylogenetic trees inferred through BI and ML recovered similar topologies (Fig. 2, Appendix 3). Individuals of the new species form a well-supported clade within a major clade containing three nominal (*Scinax cruentomma, S. strussmannae,* and *S. wandae*) and nine undescribed species. All nominal species in this major clade have a red- or brown-striped iris. The new species is recovered as sister to a clade composed of specimens from Suriname and Guyana (*Scinax* sp. clade 72), but pairwise genetic distances to them are low (mean p-distance = 1.4%) compared with the distance between other clades. We lack morphological data for these specimens, so we do not consider them as conspecific to the new species until additional data are available. *Scinax wandae* from Colombia was recovered as sister to the clade comprising the new species and the Suriname and Guyana specimens (Fig. 2).

Overall interspecific p-distance within the aforementioned major clade is 6.6%. Pairwise p-distances between the new species and other nominal species with a red- or brown-striped iris range from 2.7% (*S. wandae*) to 10.1% (*S. strussmannae;* Table 1). Intraspecific p-distances within each of these *Scinax* species range from 0% (*Scinax* sp. clade 47, *S. strussmannae* and *S. wandae*) to 0.7% (*Scinax* sp. clade 48). Average intraspecific p-distance within the new species is 0.4% and within the *Scinax* sp. clade 72 is 0.2% (Table 1).

TAXONOMIC ACCOUNT

Scinax albertinae sp. nov.
LSID: urn:lsid:zoobank.org:act:2D465FEC-21EC-4D93-829A-9730D2B7F028
White-sand's snouted treefrog
Figures 3–4, 5A, B, 6–11, 13A; Tables 1–4
Scinax sp. - Ferrão et al. (2019), Lima et al. (2021).

Holotype. INPA-H 42872 (field number APL 23058; Figs. 3A, B, 4, 5A, B, 6), adult male, collected 25 April 2020 in Rio

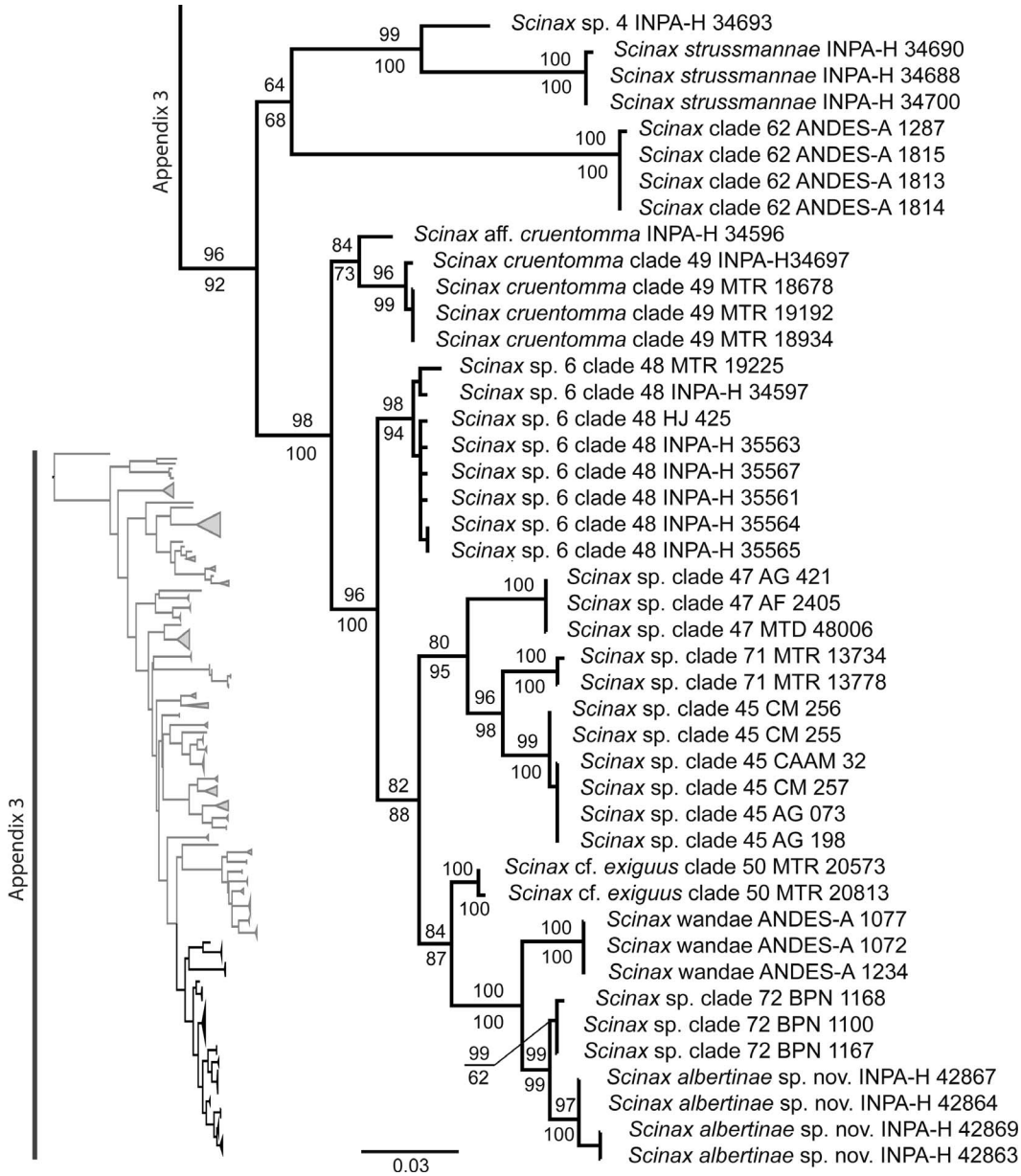

Figure 2. Bayesian phylogenetic inference focused on the major clade containing *Scinax albertinae* sp. nov. and its most closely related species, based on a fragment of the 16S rDNA mitochondrial gene. The figure at lower left depicts the complete phylogenetic tree (Appendix 3). Support values along branches represent bootstrap values of a Maximum Likelihood analysis (above) and Bayesian posterior probabilities (in %; below).

Table 1. Interspecific and intraspecific genetic distances between *Scinax albertinae* sp. nov. and closely related taxa included in our phylogenetic analyses. Uncorrected p-distances (lower diagonal) and Kimura two-parameter distances (K2P; upper diagonal) are based on a fragment of the 16S rRNA mitochondrial gene and expressed as percentages. Numbers in bold represent intraspecific p-distance values.

	Taxon	1	2	3	4	5	6	7	8	9	10	11	12	13
1	*Scinax strussmannae*	**0.0**	10.5	5.2	15.7	13.1	10.0	9.0	13.8	9.5	9.4	11.3	13.1	11.0
2	*Scinax* sp. clade 62	9.7	**0.1**	10.0	13.2	12.0	9.7	9.5	11.3	10.4	10.7	11.3	13.3	10.7
3	*Scinax* sp. 4	5.0	9.3	-	13.8	11.4	8.7	7.6	10.8	7.8	7.8	9.1	11.3	9.3
4	*Scinax* sp. clade 45	13.8	11.8	12.3	**0.1**	5.1	7.4	8.0	4.7	7.3	4.9	6.8	7.2	7.5
5	*Scinax* sp. clade 71	11.8	10.9	10.5	4.9	**0.2**	7.4	7.9	5.4	7.1	5.8	6.8	8.5	7.0
6	*Scinax cruentomma* clade 49	9.2	9.0	8.1	7.0	7.0	**0.2**	2.5	4.5	5.0	4.7	5.9	7.6	6.5
7	*Scinax* aff. *cruentomma*	8.4	8.8	7.2	7.5	7.4	2.5	-	5.4	3.3	4.1	6.7	7.6	6.4
8	*Scinax* sp. clade 47	12.4	10.3	9.9	4.6	5.2	4.3	5.1	**0.0**	5.5	4.8	6.3	6.3	6.2
9	*Scinax* sp. 6 clade 48	8.8	9.6	7.3	6.9	6.8	4.8	3.2	5.3	**0.7**	3.8	7.1	7.4	6.1
10	*Scinax* aff. *exiguus* clade 50	8.7	9.8	7.3	4.8	5.5	4.5	4.0	4.7	3.7	**0.2**	3.8	4.0	3.8
11	*Scinax wandae*	10.3	10.3	8.4	6.4	6.5	5.6	6.3	6.0	6.7	3.7	**0.0**	2.9	2.7
12	*Scinax* sp. clade 72	11.7	12.0	10.3	6.8	8.0	7.2	7.1	6.0	6.9	3.9	2.8	**0.2**	1.4
13	*Scinax albertinae* sp. nov.	10.1	9.8	8.6	7.1	6.7	6.2	6.1	5.9	5.8	3.7	2.7	1.4	**0.4**

Negro Sustainable Development Reserve (03°03′31″S, 60°45′42″W; 73 m a.s.l.), municipality of Novo Airão, Amazonas, Brazil, by M. Ferrão and A. S. Ferreira.

Paratopotypes. Nineteen adult specimens, same locality as the holotype: three males INPA-H 42867, 42863, 42857 (field numbers APL 22249, 22245, and 22243, respectively) and four females INPA-H 42861, 42868–69, 42874 (field numbers APL 22248, 22247, 22244, and 22246, respectively) collected 14 September 2018 by M. Ferrão, J. Moravec, and A. S. Ferreira; a male INPA-H 42866 (field number APL 22264) and four females INPA-H 42864, 42876, 42871, 42870 (field numbers APL 22260–63) collected 15 September 2018 by M. Ferrão, J. Moravec, and A. S. Ferreira; three males INPA-H 42862, 42865, 42875 (field numbers APL 22635–37) and a female INPA-H 42856 (field number APL 22638) collected 17 January 2019 by M. Ferrão and A. S. Ferreira; a male INPA-H 42858 (field number APL 22923) collected 10 January 2020 by A. S. Ferreira, J. Dayrell, and R. Pereira; two males INPA-H 42873, 42859 (field numbers APL 23056–57) collected 25 April 2020 by M. Ferrão and A. S. Ferreira.

Referred specimens. Same locality as the holotype. Adult female INPA-H 42968 (field number APL 22239) collected 8 June 2018 by L. J. C. L. Moraes and I. Y. Fernandes; one tadpole, Gosner stage 42, and five newly metamorphosed specimens, Gosner Stage 45 (lot INPA-H 42854, field number APL 23061), collected 25 April 2020 by M. Ferrão and A. S. Ferreira; 17 tadpoles, Gosner stages 34–38 (lot INPA-H 42855, field number APL 23059), collected 25 April 2020 by M. Ferrão and A. S. Ferreira.

Etymology. The specific epithet honors Albertina Pimentel Lima (INPA, Brazil) for her outstanding contributions to the ecology and taxonomy of Amazonian frogs and to the professional careers of many students, including most authors of this study.

Diagnosis. The new species is assigned to the genus *Scinax* based on the position of the cloacal tube in tadpoles, molecular phylogenetic relationships, and morphological similarities among adults (see comparisons). *Scinax albertinae* sp. nov. is distinguished from other congeners by the following

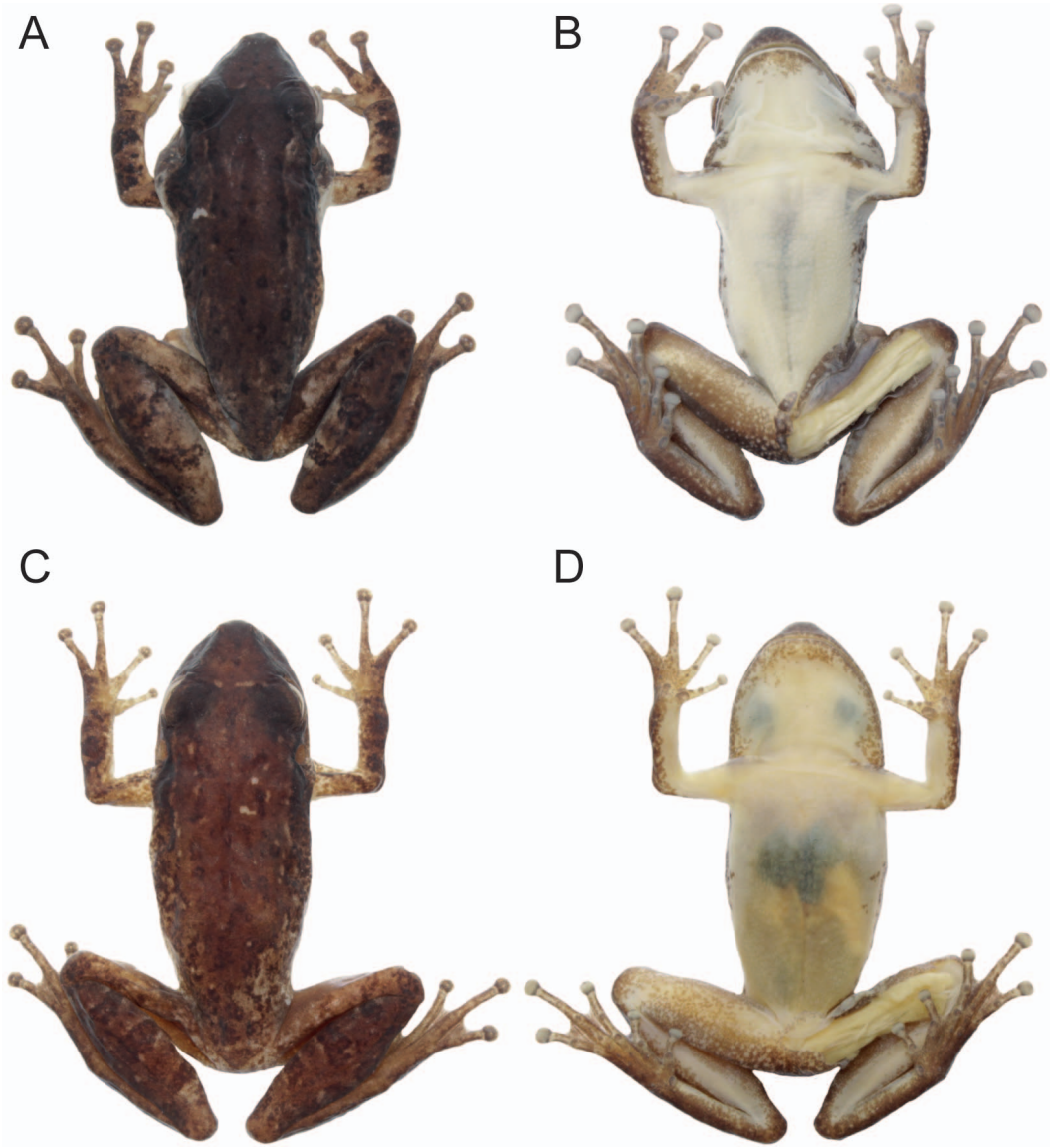

Figure 3. Dorsal and ventral views of the (A, B) male holotype INPA-H 42872 and (C, D) female paratopotype INPA-H 42871 of *Scinax albertinae* sp. nov. from Rio Negro Sustainable Development Reserve, municipality of Novo Airão, Amazonas, Brazil. Photographs: I. Y. Fernandes.

combination of characters: (1) SVL 21.6–25.4 mm ($n = 11$) in adult males and 24.8–27.0 mm ($n = 9$) in females; (2) head longer than wide; (3) snout subacuminate in dorsal view; (4) *canthus rostralis* straight in dorsal view; (5) nuptial pad present in breeding males; (6) small ulnar tubercles; (7) subarticular tubercle subconical on fingers I and II; (8) vocal sac bilobate; (9) outer metatarsal tubercle distinct and subconical; (10) small

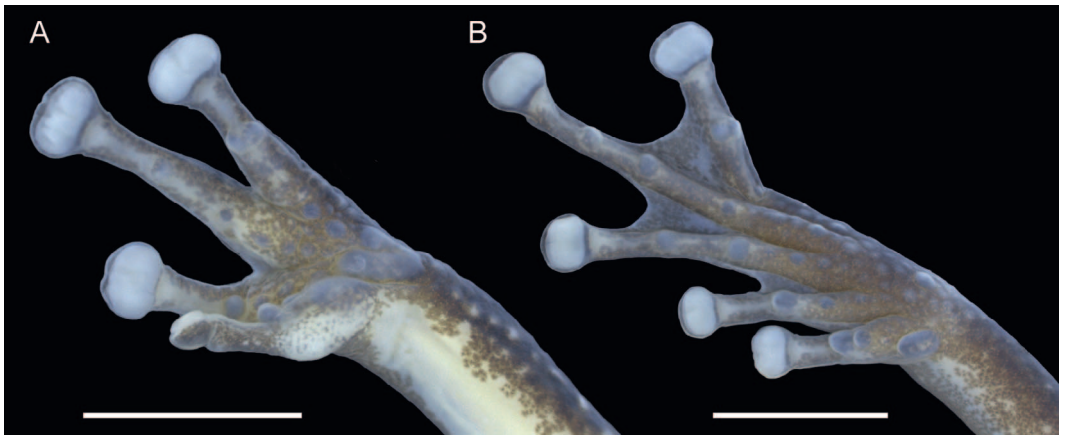

Figure 4. Ventral views of the hand (A) and foot (B) of the holotype of *Scinax albertinae* sp. nov., INPA-H 42872. Scale bar = 3 mm. Photographs: M. Ferrão.

tubercles on subcloacal region; (11) dark brown lateral stripe on flanks, fading posteriorly; (12) posterior surfaces of thigh uniformly brown; (13) horizontal bar on iris reddish-brown; (14) vocal sac with dark blotches on the lateral region; (15) absence of dark bars on thigh; (16) white bones; (17) advertisement call consisting of a single pulsed note with call duration of 502–652 ms, a call rate of 32–68 calls/min, 79–105 pulses/note, and a dominant frequency of 3,811–4,543 Hz; (18) tadpoles with brown dorsum, labial keratodont row formula 2(2)/3, keratodont row P-2 longer than P-1 and P-3, and total length reaching ~28.6 mm at Gosner stage 37.

Comparisons. Characters of compared species are enclosed in parentheses if not

Table 2. Morphometric measurements of the type series of *Scinax albertinae* sp. nov. from Rio Negro Sustainable Development Reserve, municipality of Novo Airão, state of Amazonas, Brazil. Values depict average ± standard deviation (minimum–maximum). Measurements are explained in the text.

Measurements	Males (n = 11)	Females (n = 9)
SVL	23.8 ± 1.0 (21.6–25.4)	25.8 ± 0.9 (24.8–27.0)
HL	8.8 ± 0.4 (8.2–9.3)	9.4 ± 0.4 (8.7–10.0)
HW	8.1 ± 0.4 (7.4–8.9)	8.9 ± 0.3 (8.4–9.5)
ED	2.9 ± 0.2 (2.5–3.1)	3.0 ± 0.1 (2.7–3.2)
TD	1.2 ± 0.1 (1.0–1.3)	1.3 ± 0.1 (1.1–1.4)
UEW	2.3 ± 0.1 (2.1–2.5)	2.3 ± 0.2 (2.1–2.7)
IOD	2.3 ± 0.1 (2.1–2.5)	2.5 ± 0.1 (2.4–2.7)
IND	2.0 ± 0.1 (1.9–2.1)	2.1 ± 0.1 (2.1–2.2)
END	2.9 ± 0.1 (2.6–3.0)	3.1 ± 0.1 (3.0–3.3)
HAL	6.4 ± 0.3 (6.0–6.9)	6.7 ± 0.3 (6.4–7.0)
3FD	1.1 ± 0.1 (0.9–1.3)	1.1 ± 0.1 (1.0–1.3)
4TD	1.1 ± 0.1 (0.9–1.3)	1.1 ± 0.1 (1.0–1.3)
TAL	6.8 ± 0.4 (6.1–7.3)	7.4 ± 0.2 (7.0–7.7)
FL	9.8 ± 0.5 (8.9–10.7)	10.4 ± 0.6 (9.8–11.6)
TL	12.2 ± 0.5 (11.3–13.0)	13.4 ± 0.4 (12.8–13.8)
THL	11.1 ± 0.6 (9.8–11.9)	12.1 ± 0.4 (11.5–12.8)

TABLE 3. COMPARISONS OF SPECTRAL AND TEMPORAL PARAMETERS OF THE ADVERTISEMENT CALLS OF *SCINAX ALBERTINAE* SP. NOV. AND FOUR CLOSELY RELATED SPECIES. MEASUREMENT ACRONYMS ARE DEFINED IN THE TEXT. VALUES DEPICT AVERAGE ± STANDARD DEVIATION (MINIMUM–MAXIMUM).

	Scinax albertinae sp. nov.	*Scinax cruentomma*	*Scinax exiguus*	*Scinax strussmannae*	*Scinax wandae*
Reference	Present study	Carvalho et al. (2015)	Carvalho et al. (2017)	Ferrão et al. (2018b)	Present study
Temperature (°C)	25	26.5–28.5	15–16	25	unknown
Calls analyzed	30	147	49	21	10
CD (ms)	559 ± 44 (502–652)	269 ± 22 (216–336)	1,148 ± 333 (632–1,638)	106 ± 5 (97–115)	624 ± 17 (579–639)
ICI (ms)	590 ± 207 (342–1,346)	582 ± 128 (325–1,281)	-	338 ± 93 (221–601)	577 ± 115 (391–790)
CP (ms)	1,149 ± 210 (878–1,878)	-	-	-	1,201 ± 121 (1,018–1,414)
CR (calls/min)	54 ± 8 (32–68)	-	26 ± 8 (20–35)	139 ± 24 (85–175)	50 ± 5 (42–59)
NP (pulses/call)	89 ± 7 (79–105)	47 ± 2.6 (39–54)	71 ± 8 (51–90)	24 ± 6.6 (17–30)	88 ± 2 (82–90)
PD (ms)	3.4 ± 0.7 (2–6)	-	-	2.1 ± 0.7 (2–3)	3.4 ± 0.6 (2–4)
IPI (ms)	2.9 ± 0.8 (2–7)	-	-	2.1 ± 0.4 (1–3)	3.8 ± 0.6 (3–5)
PP (ms)	6.3 ± 0.6 (5–9)	-	-	4.5 ± 0.5 (4–5)	7.2 ± 0.6 (6–8)
PRR (pulses/sec)	160 ± 14 (111–200)	175 ± 8 (154–193)	64 ± 14 (52–86)	225 ± 25 (200–250)	139 ± 11 (125–167)
LF (Hz)	2,787 ± 138 (2,551–3,052)	2,322 ± 92 (2,156–2,438)	-	2,255 ± 49 (2,213–2,441)	2,561 ± 24 (2,506–2,595)
HF (Hz)	5,396 ± 93 (5,218–5,569)	4,654 ± 157 (4,406–4,875)	-	3,696 ± 80 (3,595–3,803)	6,424 ± 33 (6,375–6,486)
DF (Hz)	4,121 ± 149 (3,811–4,543)	4,654 ± 157 (4,406–4,875)	4,522 ± 290 (4,078–5,016)	2,816 ± 93 (2,541–3,015)	5,097 ± 64 (4,952–5,146)

Table 4. Morphometric measurements, in mm, of *Scinax albertinae* sp. nov. tadpoles (lot INPA-H 42855) at distinct Gosner developmental stages. Values depict average ± standard deviation (minimum–maximum); acronyms are defined in the text.

Measurements	Stage 34 ($n = 4$)	Stage 36 ($n = 2$)	Stage 37 ($n = 10$)	Stage 38 ($n = 1$)
TMW	2.0 ± 0.1 (1.9–2.1)	2.1–2.4	2.2 ± 0.1 (2.1–2.5)	2.2
BW	5.4 ± 0.3 (5.1–5.7)	5.5–6.0	5.6 ± 0.3 (5.3–5.9)	5.4
HWLE	4.9 ± 0.2 (4.7–5.2)	5.0–5.4	5.1 ± 0.2 (4.7–5.5)	4.6
IOD	3.8 ± 0.2 (3.7–4.0)	3.9–4.0	4.0 ± 0.2 (3.7–4.3)	3.6
IND	2.0 ± 0.1 (2.0–2.1)	2.0–2.1	2.2 ± 0.0 (2.2–2.3)	2.2
BL	8.5 ± 0.3 (8.1–8.7)	8.8–9.0	8.9 ± 0.3 (8.4–9.4)	8.6
TAL	16.4 ± 1.2 (15.2–18.0)	16.0–17.5	17.8 ± 1.1 (15.8–19.5)	17.5
TTL	24.8 ± 1.1 (23.9–26.5)	24.8–26.5	26.8 ± 1.3 (24.4–28.6)	26.1
SS	5.6 ± 0.2 (5.4–5.8)	5.4–5.5	5.9 ± 0.2 (5.5–6.2)	6.0
BH	5.0 ± 0.3 (4.7–5.3)	5.2–5.5	5.5 ± 0.2 (5.2–5.8)	5.2
TMH	2.2 ± 0.1 (2.1–2.3)	2.2–2.3	2.3 ± 0.1 (2.2–2.4)	2.2
MTH	6.3 ± 0.2 (6.2–6.5)	6.5–7.0	6.8 ± 0.6 (5.9–8.0)	6.2
ED	1.8 ± 0.0 (1.8–1.9)	1.7–1.8	1.8 ± 0.0 (1.7–1.9)	1.8
END	0.8 ± 0.1 (0.7–0.9)	0.7–0.8	0.9 ± 0.1 (0.7–1.1)	0.9
NSD	1.5 ± 0.1 (1.4–1.7)	1.5–1.8	1.7 ± 0.2 (1.5–2.0)	1.8
STL	0.9 ± 0.1 (0.8–1.0)	1.0–1.1	1.0 ± 0.1 (0.9–1.3)	1.3
VTL	1.2 ± 0.1 (1.1–1.4)	1.2–1.3	1.1 ± 0.1 (0.9–1.4)	1.0
ODW	3.0 ± 0.2 (2.8–3.3)	2.8–3.0	2.9 ± 0.3 (2.4–3.5)	3.0

otherwise stated. A subacuminate snout in dorsal view and a uniformly brown posterior thigh distinguish *Scinax albertinae* sp. nov. from species of the *Scinax rostratus* group, viz., *S. garbei, S. jolyi, S. nebulosus, S. pedromedinae, S. proboscideus,* and *S. rostratus* (snout pointed or elongate in dorsal view and posterior portion of thigh spotted, marbled, or brindle; Duellman, 1972a; Duellman and Wiens, 1992, 1993; Lescure and Marty, 2000).

A SVL of 21.6–25.4 mm in adult males distinguishes *S. albertinae* sp. nov. from the large species *S. boesemani* (28.4–31.8 mm; Duellman, 1986), *S. chiquitanus* (27.9–33.3 mm; Duellman and Wiens, 1993), *S. funereus* (29.8–36.9 mm; Duellman, 1971; Duellman and Wiens, 1993), *S. fuscovarius* (36–54 mm; Goldberg et al., 2018), *S. iquitorum* (35.0–38.5 mm; Moravec et al., 2009), *S. karenanneae* (26.6–28.9 mm; Pyburn, 1993); *S. onca* (31.3–34.5 mm; Ferrão et al., 2017), *S. oreites* (28.4–33.5 mm; Duellman and Wiens, 1993), *S. ruber* (29.4–41.2 mm; Duellman and Wiens, 1993), *S. sateremawe* (35.2–38.1 mm; Sturaro and Peloso, 2014), and *S. x-signatus* (34.5–38.4 mm; Araujo-Vieira et al., 2020).

A reddish-brown horizontal bar on the iris and the subacuminate snout in dorsal view distinguish *S. albertinae* sp. nov. from *S. ruberoculatu*s (upper portion of iris red and horizontal dark brow absent, snout truncate in dorsal view; Ferrão et al., 2018a). In addition, tadpoles of *S. albertinae* sp. nov. differ from those of *S. ruberoculatus* by the presence of a dark brown horizontal stripe on the iris (horizontal stripe on iris absent; Ferrão et al., 2018a).

Presence of a bilobate vocal sac in males distinguishes *S. albertinae* sp. nov. from *S. fuscomarginatus, S. madeirae,* and *S. villasboasi* (single vocal sac; Brusquetti et al., 2014). In addition, a wider head in males and females, HW/SVL = 34 ± 1%, distinguishes *S. albertinae* sp. nov. from *S. fuscomarginatus* (28 ± 2%), *S. madeirae* (30 ± 1%), and *S. villasboasi* (30 ± 1%; Brusquetti et al.,

2014). The advertisement call of *S. albertinae* sp. nov. also differs from those of *S. madeirae* in call duration of 502–652 ms (720–1,160 ms; Brusquetti et al., 2014).

Scinax albertinae sp. nov. can be distinguished from *S. baumgardneri* by SVL in males, 21.6–25.4 mm, and females, 24.8–27.0 mm; snout subacuminate in dorsal view; *canthus rostralis* straight; and outer metatarsal tubercle distinct and subconical (SVL 29.0 mm in the male holotype and 29.5–32.0 mm in females, snout truncate in dorsal view, *canthus rostralis* rounded, outer metatarsal tubercle indistinct; Rivero, 1961).

Scinax albertinae sp. nov. can be distinguished from *S. blairi* by SVL in males, 21.6–25.4 mm, and females, 24.8–27.0 mm, and by the absence of dark bars on the thigh (SVL 27.8–30.1 mm in males and 32.1–32.5 mm in females, 1–3 dark bars on thigh; Fouquette and Pyburn, 1972). In addition, the advertisement call of *S. albertinae* sp. nov. consists of a single note with a call duration of 502–652 ms and 79–105 pulses/note (call duration 140–160 ms, 18–22 pulses/note; Fouquette and Pyburn, 1972).

Scinax albertinae sp. nov. can be distinguished from *S. lindsayi* by the subconical subarticular tubercle on fingers I and II; the dark lateral stripe on the dorsum, which fades posteriorly; and the white nuptial pad in breeding males (subarticular tubercle rounded on all fingers, dark lateral stripe and nuptial pad absent; Pyburn, 1992). In addition, the advertisement call of *S. albertinae* sp. nov. lasts 502–652 ms and has a dominant frequency of 3,811–4,543 Hz (call duration 80–100 ms, dominant frequency 2,695–3,235 Hz; Pyburn, 1992).

Scinax albertinae sp. nov. can be distinguished from *S. cruentomma* by the maximum SVL in males, 25.4 mm, and females, 27.0 mm; *canthus rostralis* straight; nuptial pad present in breeding males; bilobate vocal sac; small subcloacal tubercles; reddish-brown horizontal bar on iris; and white bones (maximum SVL 27.7 in males and 30.6 in females, *canthus rostralis* rounded, nuptial pad absent in breeding males, single vocal sac, subcloacal tubercles absent, bright red horizontal bar on iris, green bones; Duellman, 1972b). In addition, the advertisement call of *S. albertinae* sp. nov. differs from that of *S. cruentomma* in call duration, 502–652 ms, and dominant frequency, 3,811–4,543 Hz (call duration 350–370 ms, dominant frequency 3,200–3,400 Hz at the type locality in Ecuador; call duration 216–336 ms, dominant frequency 2,156–2,438 Hz at the upper Negro River in Brazil; Duellman, 1972b; Carvalho et al., 2015). Tadpoles of *S. albertinae* sp. nov. differ from those of *S. cruentomma* in having a brown dorsum, labial keratodont row formula 2(2)/3, and maximum total length ~28.6 mm only at Gosner stage 37 (pale olive-tan dorsum, labial keratodont row formula 2(2)/3(1), maximum total length 28.2 mm at Gosner stage 30; Duellman, 1972b).

Scinax albertinae sp. nov. can be distinguished from *S. exiguus* by the SVL in males, 21.6–25.4 mm, and females, 24.8–27.0 mm; ulnar tubercles present; moderate-sized vocal sac; and TD/ED = 37–44% in males (SVL 18–20.8 mm in males and 20.1–24.5 mm in females, ulnar tubercles absent, large vocal sac, and TD/ED = 48–60% in males; Duellman, 1986). The advertisement call of *S. albertinae* sp. nov. has a call duration of 559 ± 44 ms, 89 ± 7 pulses/call, and a call rate of 54 ± 8 calls/min (call duration 1,148 ± 333 ms, 71 ± 8 pulses/call, and call rate 26 ± 8 calls/min at the type locality; Duellman, 1986; Carvalho et al., 2017).

Scinax albertinae sp. nov. can be distinguished from *S. strussmannae* by the SVL in males, 21.6–25.4 mm; snout subacuminate in dorsal view; *canthus rostralis* straight; reddish brown horizontal bar on iris; and vocal sac with dark blotches restricted to the

lateral region (SVL 20.2–22.5 mm in males, snout truncate in dorsal view, *canthus rostralis* curved, bright red horizontal bar on iris, vocal sac immaculate bright yellow; Ferrão et al., 2018b). The advertisement call of *S. albertinae* sp. nov. is distinct from that of *S. strussmannae* in its call duration of 502–652 ms, call rate of 32–68 calls/min, 79–105 pulses/note, and dominant frequency of 3,811–4,543 Hz (call duration 97–115 ms, call rate 85–175 calls/min, 23–27 pulses/note, and 2,541–3,015 Hz; Ferrão et al., 2018b).

Scinax albertinae sp. nov. can be distinguished from *S. wandae* by the absence of a well-defined and continuous dark dorsolateral stripe, maximum SVL 25.5 mm in males, white nuptial pad present in breeding males, *canthus rostralis* straight and bilobate vocal sac (well-defined and continuous dark dorsolateral stripe always present, maximum SVL 26.9 mm in males, nuptial pad absent, *canthus rostralis* rounded, and single vocal sac; Pyburn and Fouquette, 1971). The advertisement call of *S. albertinae* sp. nov, with a call duration of 502–652 ms (average 559 ± 44 ms) and a dominant frequency of 3,811–4,543 Hz, differs from the calls of *S. wandae* at its type locality (call duration 653–696 ms, dominant frequency 4,800–5,050 Hz; Pyburn and Fouquette, 1971) and at San Martín, Meta, Colombia (average call duration 624 ± 17 ms, dominant frequency 4,800–5,050 Hz; Table 3).

Holotype description. INPA-H 42872 (field number APL 23058), an adult male (Fig. 3A, B), SVL 23.8 mm. Head longer than wide (HL/HW = 1.1); head length and width 36% and 34% of SVL, respectively. Snout subacuminate in dorsal view, rounded in lateral view; eye–nostril distance 35% of HL; nostrils protruding, nostril opening directed dorsolaterally; internarial region barely concave; *canthus rostralis* well-defined, straight in dorsal view; loreal region concave. Eyes large, protruding laterally; eye diameter equals eye–nostril distance (ED/END = 1.0) and about 35% of HL; upper eyelid 110% of IOD. Interorbital region flattened; interorbital distance about 28% of head width. Tympanum distinct and vertically ovoid; upper portion obscured by the supratympanic fold; tympanum diameter 40% of eye diameter. Supratympanic fold well-defined, extends from anterior portion of tympanum to upper arm insertion. Vocal slits present, extend from the angle of the jaw to the lateral base of the tongue, not covered by the lateral margin of the tongue. Tongue ovoid, entirely attached to the floor of the mouth. Dentigerous processes of vomers triangular and pronounced, separated from each other by 1/3 of their width, each with three evident teeth. Choanae oval. Vocal sac of moderate size, bilobate and subgular, when inflated extends from the subgular region to the upper arm insertion.

Arms slender, forearm more robust than upper arm. Axillary membrane absent (Fig. 3A, B). Ulnar tubercles low, distributed from elbow to lateral base of finger IV. Hand length about 26% of SVL; relative length of fingers I < II < IV < III; vestigial webbing only between fingers II and III (Fig. 4A); lateral fringes present on all fingers, but poorly developed; finger discs elliptical, wider than long; finger III disc wider than tympanum diameter (3FD/TD = 1.1); finger I disc smaller than others. Subarticular tubercles single and subconical on fingers I and II, single and rounded on finger III, and bifid on finger IV; supernumerary tubercles flattened on the base of fingers II–IV, subconical on the base of finger I; palmar tubercle bifid and flat; thenar tubercle oval and flat. Nuptial pad white, covers the thumb dorsolaterally from the level of the subarticular tubercle to the proximal base of the thenar tubercle.

Hind limbs slender and long; THL + TL about 97% of SVL; tibia longer than thigh

(TL/THL = 1.1); thigh and tibia length 47% and 50% of SVL, respectively. Tubercles on knee absent. Foot length about 40% of SVL and 140% of tarsus length. Tarsal fold absent; tarsal tubercles small and low, less evident than ulnar tubercles. Toes slender (Fig. 4B); relative length of toes I < II < III < V < IV; toe discs elliptical, wider than long; disc on toe IV slightly larger than that on finger III (4TD/3FD = 1.03); discs on toes I and II wider than those on other toes; subarticular tubercle bifid on toe V, single and subconical on toes I–IV; toe webbing formula I vestigial II 2^{-}–3^{-} III $1^{1/2}$–3^{-} IV 3–$1^{1/2}$ V; lateral fringes present on all toes; supernumerary tubercles rounded and evident; inner metatarsal tubercle oval and protuberant; outer metatarsal tubercle small, subconical and about two times smaller than the inner tubercle. Cloacal opening at the upper level of thighs; small subcloacal tubercles present.

In life, skin on upper eyelids, flanks, and dorsal surfaces of body, forearm, and tibia finely granulate with several scattered tubercles; dorsal surface of the head mostly smooth with few scattered tubercles; upper arm and thigh smooth (Fig. 5A). Vocal sac smooth. Chest, belly, and ventral surface of thigh areolate. In preservative, dermal tubercles barely evident.

Holotype measurements (in mm). SVL, 23.8; HL, 8.6; HW, 8.0; ED, 3.0; TD, 1.2; UEW, 2.5; IOD, 2.3; IND, 2.1; END, 3.0; HAL, 6.3; 3FD, 1.3; THL, 11.2; TL, 11.9; FL, 9.5; TAL, 6.9; 4TD, 1.3.

Coloration of holotype in life. At night (Fig. 5A, B), the dorsal surface of the snout is brownish cream, with a longitudinal medial dark brown line that extends from the internarial area to the level of two dark brown tubercles that lie between anterior corners of the eyes; a brown W-shaped mark at the anterior edge of the interorbital region is bordered laterally by a light grey stripe; a dark brown canthal stripe extends from the tip of the snout to the anterior corner of each eye; loreal region dark brown; infra-ocular region cream. Iris tan with a horizontal reddish-brown stripe. Dorsum light yellowish brown with scattered dark brown tubercles; a dorsolateral brownish cream stripe that runs from the posterior margin of the eye is conspicuous anteriorly but fades posteriorly; a lateral dark brown stripe starts as a narrow supratympanic stripe from the posterior corner of each eye, widens above the upper arm insertion, and fades posteriorly; flanks pale yellow. Dorsal surfaces of forearm, tibia, and tarsus light brown; ulnar tubercles cream; two transverse brown stripes on forearm and three on tibia; dorsal surface of thigh yellowish brown, anterior and posterior surfaces brown; cloacal region yellowish cream. Vocal sac bright yellow with dark brown melanophores distributed laterally; chest and belly yellowish cream; ventral surfaces of hand, forearm, thigh, tarsus, and foot light brown; ventral surface of tibia translucent ventrally, pale brown laterally.

Coloration of holotype in preservative. Dark stripes and marks on head, dorsum, forearm, and thigh remain visible (Fig. 3A, B). The dorsolateral stripe is clear and more conspicuous. Cream and yellow surfaces on venter are white.

Vocalization. The advertisement call of *Scinax albertinae* sp. nov. consists of a single pulsed note emitted in series of 11 ± 4 calls (5–20; $n = 13$; Fig. 6A, B). Calls have an average duration of 559 ± 44 ms (502–652 ms; $n = 30$), an intercall interval of 590 ± 207 ms (342–1,346 ms; $n = 30$), and a call period of 1,149 ± 210 ms (878–1,878 ms; $n = 30$). Calls are emitted at an average rate of 54 ± 8 calls/min (32–68 calls/min; $n = 30$). On average, calls are composed of 89 ± 7 pulses (79–105 pulses; $n = 30$). Pulses have an average duration of 3.4 ± 0.7 ms (2–6 ms; *n*

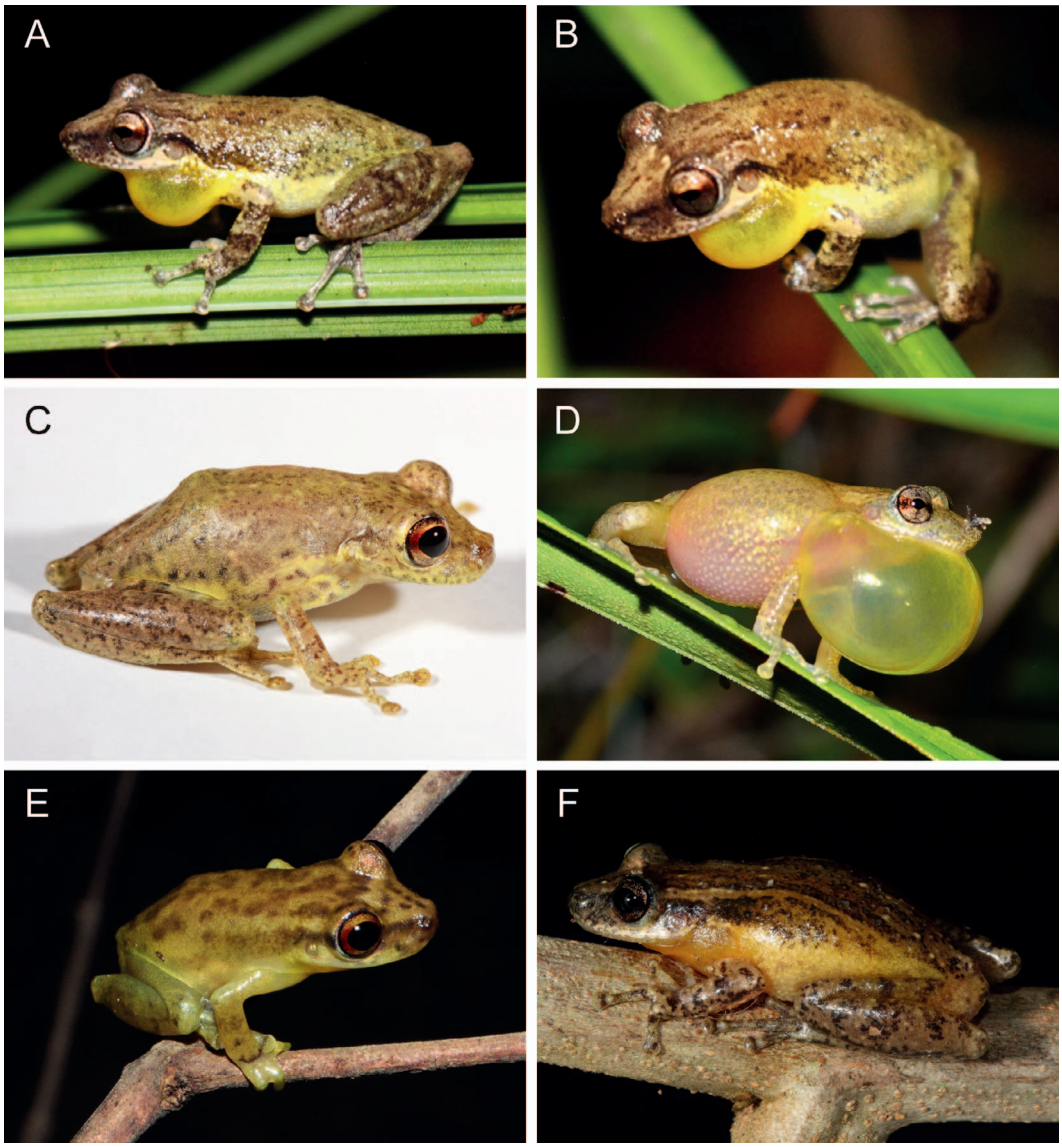

Figure 5. Live specimens of *Scinax albertinae* sp. nov. (A–B) and closely related species (C–F). (A–B) Male holotype, INPA-H 42872, RDS Rio Negro, Amazonas, Brazil. (C) *Scinax cruentomma,* QCAZ 43772, adult female from Francisco de Orellana, Orellana, Ecuador. (D) *Scinax exiguus,* unvouchered male from Tepequém, Roraima, Brazil. (E) *Scinax strussmannae*, INPA-H 34688, male holotype from Tapauá, Amazonas, Brazil. (F) *Scinax wandae,* IAvH-Am 15107, male from La Macarena, Meta, Colombia. Photographs: A. S. Ferreira (A–B), S. Ron, bioweb.bio (C), I. Y. Fernandes (D), R. de Fraga (E), and A. R. Acosta-Galvis (F).

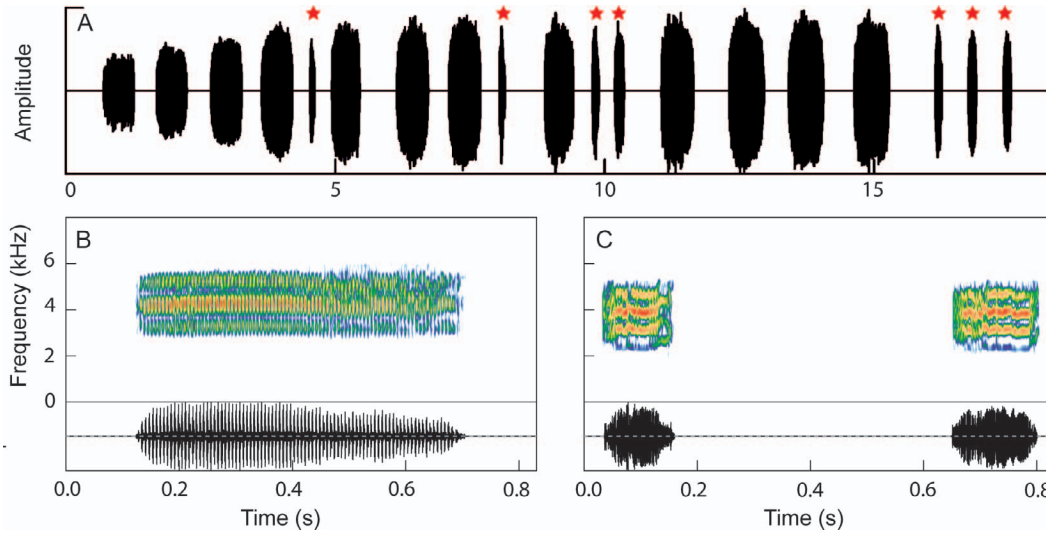

Figure 6. Vocalization of the holotype of *Scinax albertinae* sp. nov. (A) Call series with 12 advertisement calls, detailed in (B), are interleaved with 7 territorial calls (red stars), detailed in (C).

= 77) and an interpulse duration of 2.9 ± 0.8 ms (2–7 ms; $n = 77$). An average pulse lasts for 6.3 ± 0.6 ms (5–9 ms; $n = 77$). Pulses are emitted at an average rate of 160 ± 14 pulses/sec (111–200 pulses/sec; $n = 77$). Calls have three distinct frequency bands; the dominant frequency always corresponds to the central one, which averages 4,121 ± 149 Hz (3,811–4,543 Hz; $n = 30$). The average low frequency is 2,787 ± 138 Hz (2,551–3,052 Hz; $n = 30$) and the average high frequency is 5,396 ± 93 Hz (5,218–5,569 Hz; $n = 30$). See Table 3 for complete values of acoustic parameters measured for the three recorded males.

The territorial call consists of a single tonal note with a call duration of 115 ± 26 ms (72–168 ms; $n = 15$; Fig. 6C). Calls are usually emitted within an advertisement call series ($n = 11$), rarely succeeding ($n = 3$) or preceding ($n = 1$) it. Territorial calls have an average intercall interval of 550 ± 228 ms (299–1,091 ms; $n = 15$), an average call period of 666 ± 237 ms (405–1,219 ms; $n = 15$), and are emitted at a rate of 99 ± 31 calls/min (49–148 calls/min; $n = 15$). On average, 3–4 distinct frequency bands (3.2 ± 0.4; $n = 15$) were observed in the territorial calls. The dominant frequency, 3,748 ± 307 Hz (3,143–4,522 Hz; $n = 15$), usually corresponds to the second frequency band ($n = 14$). The average low frequency is 2,736 ± 216 Hz (2,323–3,083 Hz; $n = 15$) and the average high frequency is 4,792 ± 256 Hz (4,124–5,233 Hz; $n = 15$).

Variation. Morphometric variation of the paratopotypes is summarized in Table 2. External morphology mostly agrees with the holotype. Subarticular tubercle on finger IV is bifid in 74% of specimens, slightly bifid in 21%, and rounded in 5%. Subarticular tubercle on toe V is bifid in 42% of specimens, slightly bifid in 26%, and rounded in 32%. Expanded vocal sac and nuptial pads are absent in adult males collected in the nonbreeding season (56%). Number and presence of teeth varies from 1 to 5 on the right odontophore and from 1 to

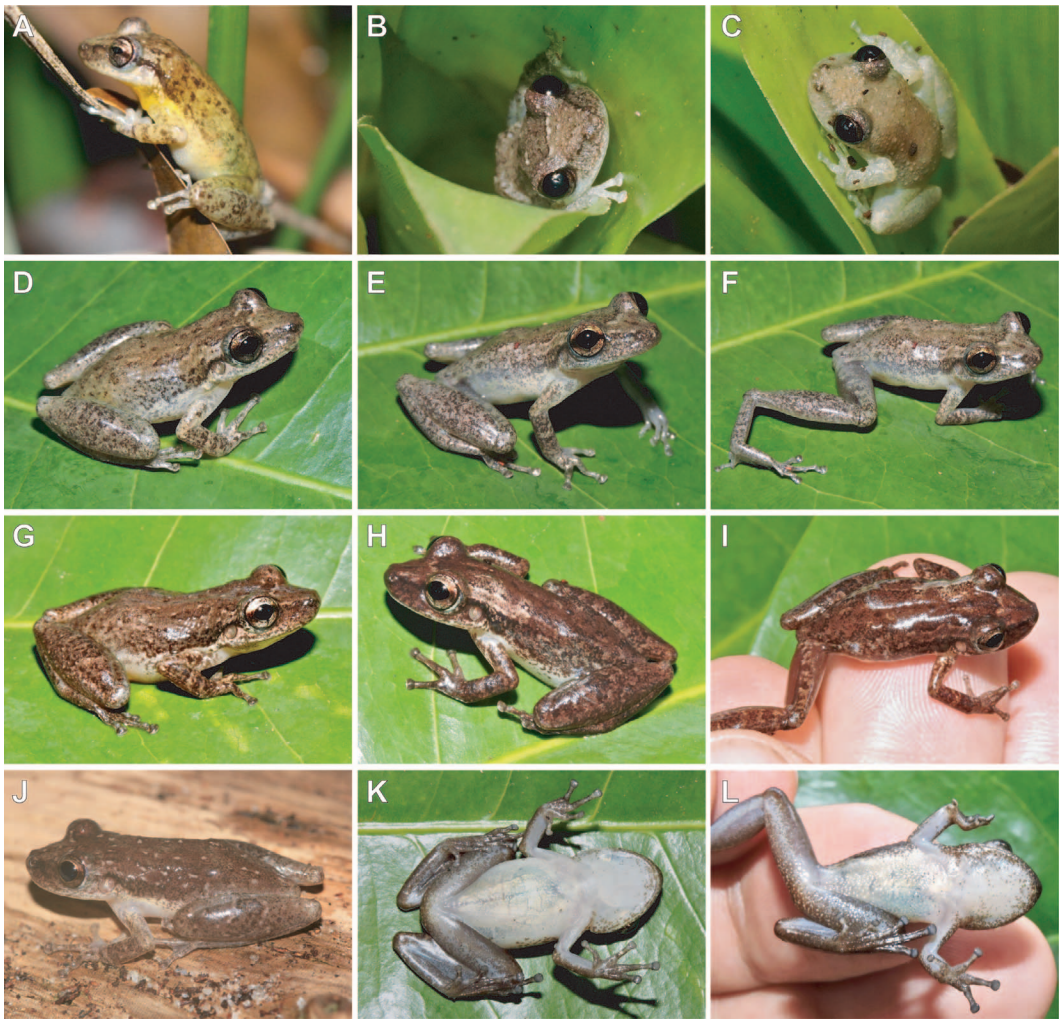

Figure 7. Coloration in life of *Scinax albertinae* sp. nov. paratopotypes and the referred specimen. Nocturnal pattern: (A) Male, INPA-H 42873, SVL = 24.4 mm. (B, C) Male, INPA-H 42857, SVL = 25.4 mm. (D) Male, INPA-H 42867, SVL = 23.3 mm. (E, F) Female, INPA-H 42869, SVL = 24.8 mm. Diurnal pattern: (G) INPA-H 42867. (H, I) INPA-H 42869. (J) Female, INPA-H 42968, SVL unmeasured. (K) INPA-H 42869. (L) Female, INPA-H 42868, SVL = 26.6 mm. Photographs: A. S. Ferreira (A), J. Moravec (B–I, K and L) and L. J. C. L. Moraes (J).

6 on the left odontophore; male specimen INPA-H 42873 lacks teeth on both odontophores.

Although dark brown marks are evident in specimens during both day and night, overall external color changes markedly between these periods (Fig. 7). The nocturnal yellow-brownish color changes to darker brown tones during the day (Fig. 7G–J). Variation in overall coloration is also evident between distinct rainfall periods, likely correlated with the reproductive cycle of the species. During the rainy season, when the species reproduces, specimens show a more yellow-

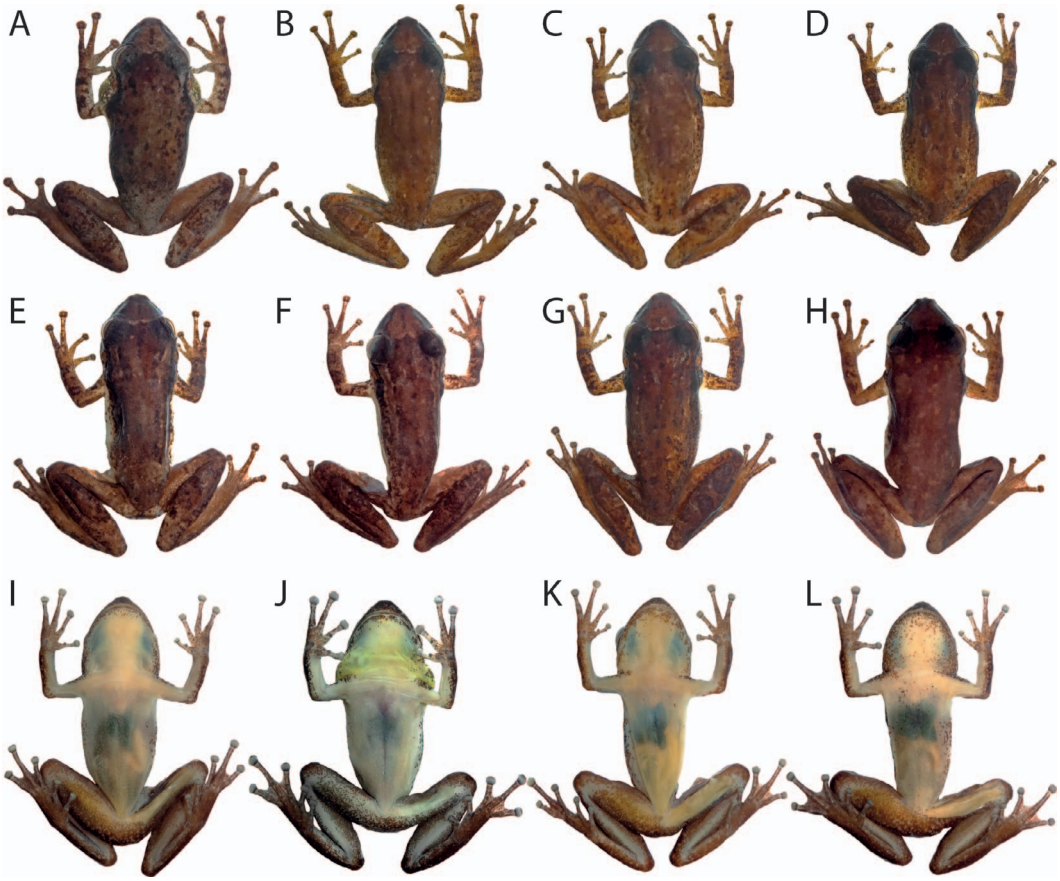

Figure 8. Dorsal and ventral views of *Scinax albertinae* sp. nov. paratopotypes. (A) Male, INPA-H 42873, SVL = 24.4 mm. (B) Female, INPA-H 42861, SVL = 26.2 mm. (C) Female, INPA-H 42870, SVL = 27.0 mm. (D) Male, INPA-H 42867, SVL = 23.3 mm. (E) Male, INPA-H 42863, SVL = 23.4 mm. (F) Female, INPA-H 42869, SVL = 24.8 mm. (G) Male, INPA-H 42857, SVL = 25.4 mm. (H) Male, INPA-H 42866, SVL = 23 mm. (I) Male, INPA-H 42857. (J) Male, INPA-H 42873. (K) INPA-H 42869. (L) Male, INPA-H 42868, SVL = 24.9 mm. Photographs: M. Ferrão.

ish dorsum (Figs. 5A, B, 7A). During the dry season, specimens became paler, with a yellowish-grey or yellowish-brown coloration (Fig. 7B–F). Skin texture also varies between dry and rainy seasons, with granules more evident during the former season (Fig. 7B, C) and a smoother appearance during the latter (Fig. 7D–J).

In preservative, light grey dorsal spots are present in 63% of specimens (Fig. 8). Interorbital marks are present in all specimens except INPA-H 42876, 42856, and 42859. In 42% of specimens, this interorbital mark is formed by a dark brown mark bordered anteriorly by a light grey mark, whereas only a light grey mark is evident in 37% of specimens and only a dark brown mark is evident in 5% of specimens. One-to-three dark brown bars are present on the tibia in 68% of specimens; they are absent in 32% of specimens. A dark brown dorsolateral stripe formed by blotches and spots is present in 37% of specimens but absent in the remaining ones. The vocal sac is cream to

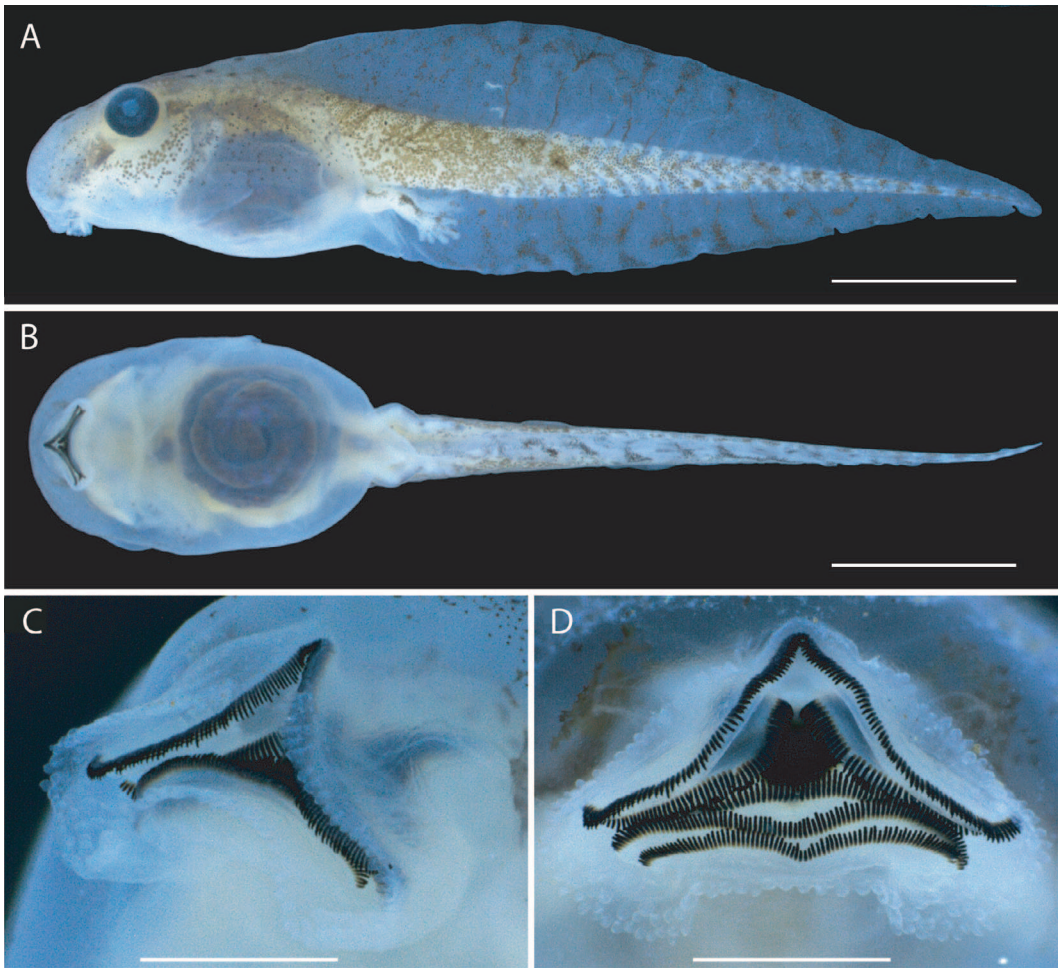

Figure 9. Preserved tadpole of *Scinax albertinae* sp. nov. (lot INPA-H 42855), Gosner stage 37. (A) Lateral and (B) ventral views, and (C) lateroventral and (D) ventral views of the oral disc. Scale bars = 5 mm (A, B) and 1 mm (C, D).

white in the most recently collected males (INPA-H 42873, 42859); in five females, dark melanophores are randomly distributed in the central portion of the gular region (INPA-H 42856, 42861, 42864, 42868, and 42876). Chest and belly are immaculate cream in all specimens except two females that have small dark brown blotches on the belly (INPA-H 42868 and 42876).

Tadpoles. Description was based on 17 tadpoles (lot INPA-H 42855) at stages 34 to 38 (Figs. 9, 10). Total length 26.8 ± 1.3 mm (24.4–28.6 mm; $n = 10$; Table 4). Body triangular in lateral view, ovoid in dorsal view; body length 33% ± 1% (32–35%) of total length; body longer than high (BL/BH = 1.6 ± 0.0, 1.6–1.7) and as wide as high (BW/BH = 1.0 ± 0.0, 1.0–1.1). Snout rounded in dorsal and lateral views. Nostrils rounded, dorsally positioned and directed; internarial region flattened; internarial distance 54% ± 3% (51–59%) of interorbital

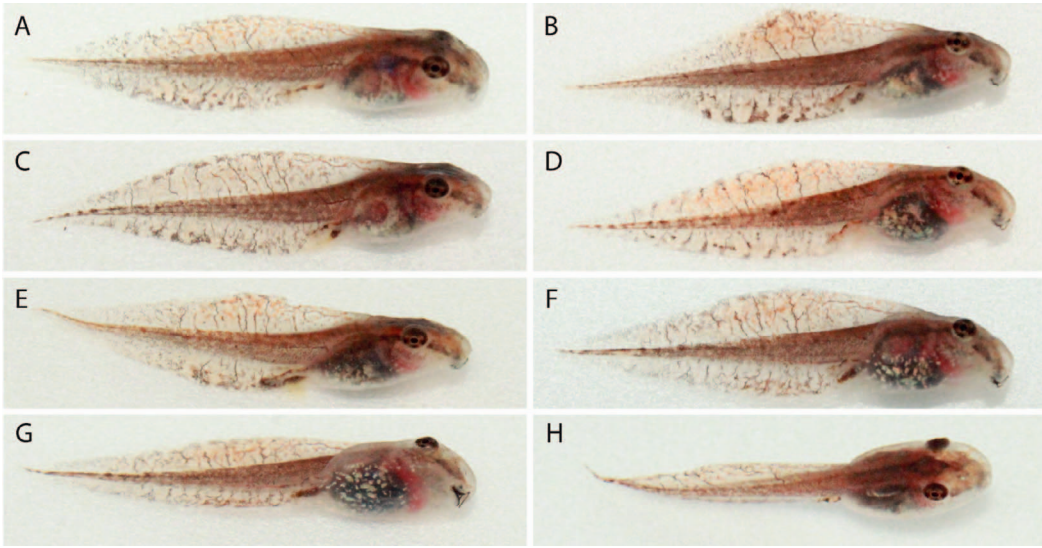

Figure 10. Coloration in life of tadpoles of *Scinax albertinae* sp. nov. (lot INPA-H 42855), Gosner stage ~ 37. Photographs: M. Ferrão.

distance and 39% ± 2% (36–41%) of body width. Eyes positioned and directed dorsolaterally, marginally visible in ventral view; eye diameter 20% ± 1% (19–22%) of body length and 31% ± 2% (30–34%) of snout–spiracle distance; interorbital region flattened, interorbital distance 72% ± 4% (68–79%) of body width. Spiracle sinistral, positioned at an angle of approximately 30°, opening directed posterodorsally, inner wall free from body. Tail long and unflagellated, twice as long as the body (TAL/BL = 2.0 ± 0.1, 1.8–2.1; $n = 10$); tail length 67% ± 1% (65–68%) of total length; tail higher than body height (MTH/BH = 1.3 ± 0.1, 1.1–1.4); upper fin higher than lower fin. On average, tail muscle as high as wide (TMH/TMW = 1.0 ± 0.1, 0.9–1.1); tail muscle height 34% ± 3% (30–38%) of maximum tail height and 26% ± 1% (24–27%) of body height (Table 4).

Oral disc situated and directed anteroventrally, protuberant; oral disc width 53% ± 5% (44–61%) of body width. Upper lip unemarginated laterally; lower lip emarginated laterally. Papillae rounded and long; uniseriate row of marginal papillae on upper lip, with a moderate gap anteriorly; biseriate and uniseriate rows of marginal papillae on the lateral fold and on the central portion of lower lip, respectively; marginal papillae row formula (1)/2/1. Submarginal papillae present on the lateral fold. Jaw sheaths serrated with conical cusps; upper jaw sheath M-shaped; lower jaw sheath V-shaped. Labial keratodont row formula 2(2)/3; A-1 slightly longer than A-2; a narrow gap in A-2; P-1 and P-3 approximately same length, P-2 longer than P-1 and P-3.

In life, tadpoles of *Scinax albertinae* sp. nov. at stage 37 have a light brown snout that is translucent anteriorly; the dorsum is brown with a dark brown interorbital mark (Fig. 10). On the snout, a dark brown lateral stripe runs from the level of the lower labium to the eye; the infraorbital region is white. The iris is brownish orange with a horizontal dark brown stripe; there are dark brown

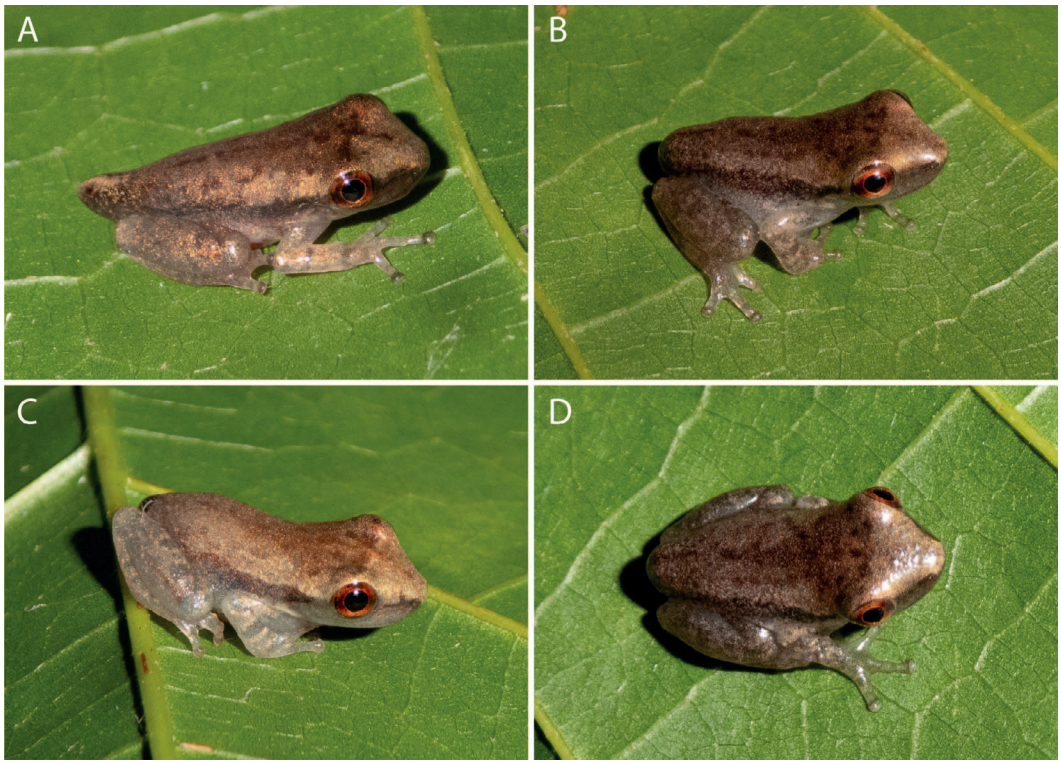

Figure 11. Color in life of metamorphs of *Scinax albertinae* sp. nov. (lot INPA-H 42854), Gosner stage 45. Photographs: M. Ferrão.

blotches on the upper and lower edges of the iris, but they do not form a complete vertical stripe. A dark brown lateral stripe extends from the posterior eye corner to the level of the tail–muscle insertion. Tail muscle is brown with several tiny light spots (Fig. 10); a thin dark brown lateral line runs from the base of the tail muscle to the tail tip and is more conspicuous posteriorly. Dorsal and ventral fins are translucent cream with dark brown vermiculation, dark melanophores, and orange blotches; there are dark brown blotches on the upper and lower edges of the central region of the fins (Fig. 10). Venter is translucent with several silvery spots on the intestinal region (Fig. 10).

In life, metamorphs at stage 45 (lot INPA-H 42854) have a tan dorsum with light to dark brown marks, including interorbital stripes and blotches (Fig. 11). There is a dark brown canthal stripe; the loreal region is dark brown. A dark brown lateral stripe extending from the posterior corner of the eye to the groin is more conspicuous anteriorly. Lower portions of the flanks are greyish white. Dorsal surfaces of limbs are light tan; one-to-three grey bars are present in some individuals (Fig. 11). The iris is reddish orange with a dark brown horizontal stripe. Ventral surface is translucent with silver blotches.

Geographic distribution and habitat. *Scinax albertinae* sp. nov. is known only from the type locality in the RDS Rio Negro. All individuals were recorded exclusively in white-sand forest (*campinarana*), which is

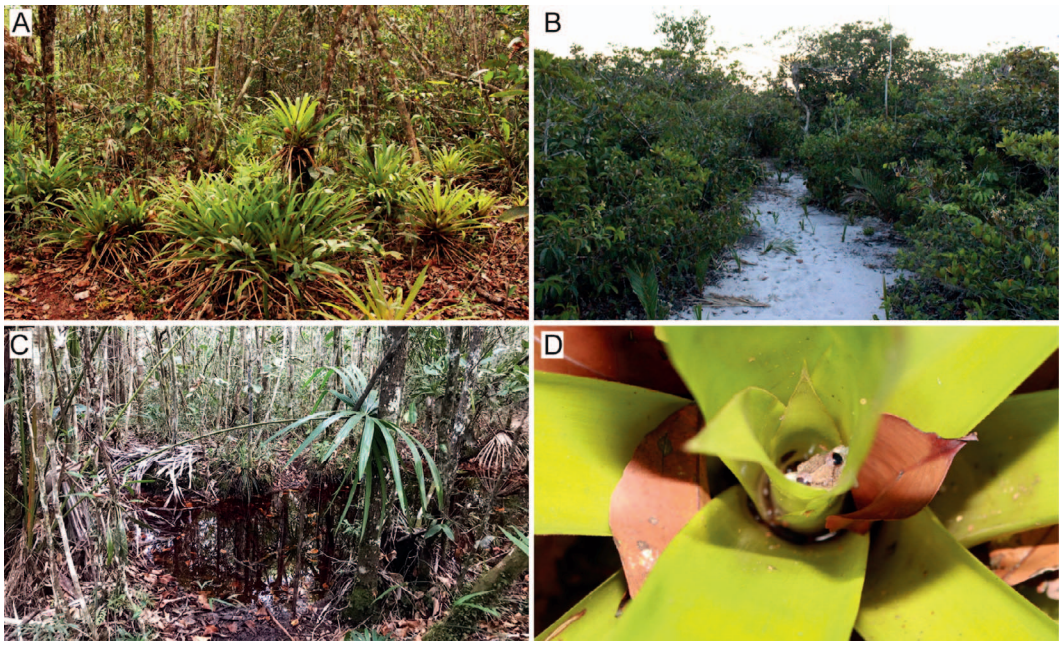

Figure 12. White-sand ecosystems in the Rio Negro Sustainable Development Reserve, municipality of Novo Airão, state of Amazonas, Brazil, the type locality of *Scinax albertinae* sp. nov. (A) White-sand forest with canopy below 20 m—*campinarana*—with several bromeliads. (B) Open white-sand forest with canopy below 10 m—*campina*. (C) Temporary pool filled with dark, acidic waters used as breeding sites by *Scinax albertinae* sp. nov. (D) An unvouchered specimen of *Scinax albertinae* sp. nov. hidden in a bromeliad during the dry season. Photographs: A. S. Ferreira.

characterized by a canopy height below 20 m (Fig. 12A). Extensive sampling efforts were conducted in other habitats that contribute to the landscape mosaic of the RDS Rio Negro, including open white-sand forest (*campina,* with canopy height below 10 m; Fig. 12B) and dense forests with rich soils, but the new species was never observed in them. Thus *S. albertinae* sp. nov. appears to be typical of WSE but likely inhabits only a single habitat within these ecosystems. This hypothesis is supported by the fact that *S. albertinae* sp. nov. also has never been recorded in dense forests geographically close to RDS Rio Negro, in Manaus and northern Purus–Madeira interfluve, despite our long-term sampling effort in those regions.

During the dry season, we observed individuals of *Scinax albertinae* sp. nov. hidden in bromeliads (*Guzmania brasiliensis;* Fig. 12D) or in plastic tubes used to mark sampling trails in the RDS Rio Negro sampling module. This indicates that phytotelmata may represent important refuges for this species. During the rainy season, individuals were recorded active and more exposed, usually over shrub vegetation near large temporary pools (Fig. 12C). Although the closest relatives of *S. albertinae* sp. nov. are explosive breeders (e.g., *S. strussmannae;* Ferrão et al., 2018b), based on our field observations this new species is likely a prolonged breeder (*sensu* Wells, 1977): we recorded males calling for several consecutive days in the rainy season and females

were not observed arriving synchronously with males. Males call while perched horizontally or vertically on leaves and small trunks near temporary pools not connected to streams, where we also recorded tadpoles. These pools were filled with dark, acidic water formed by the accumulation of organic material following incomplete decomposition in the surrounding sandy soil.

Two other hylid species were heard near the temporary pools used as breeding sites by *Scinax albertinae* sp. nov.: *Osteocephalus vilarsi* and *Trachycephalus cunauaru* Gordo, Toledo, Suárez, Kawashita-Ribeiro, Ávila, Morais and Nunes, 2013. Yet, the only other anuran species actually observed using the same pools to breed is the microhylid *Chiasmocleis hudsoni* Parker, 1940, whose tadpoles were recorded with those of *S. albertinae* sp. nov.

DISCUSSION

Scinax albertinae is the third hylid frog associated with WSE of Central Amazonia. The other two are *Trachycephalus venezolanus* (Mertens, 1950) and *Osteocephalus vilarsi* (Carvalho et al., 2018; Ferrão et al., 2019). Moreover, molecular, morphologic, and bioacoustic data recover at least two additional candidate species of *Adenomera* (Leptodactylidae) and *Rhinella* (Bufonidae) that are associated with this environment at RDS Rio Negro (A. P. Lima, unpublished data). These associations, together with results of other studies of species diversity of WSE in Central Amazonia that consider anurans (Carvalho et al., 2018; Ferrão et al., 2019), reptiles (Fraga et al., 2018; Ferreira et al., 2019), birds (Borges et al., 2001; Almeida, 2016), dipterans (Ale-Rocha and Vieira, 2008), and plants (Terra-Araujo et al., 2015; Gaem et al., 2019), highlight the extreme biological significance and uniqueness of this area, which until recently has been largely overlooked.

Scinax albertinae is known only from its type locality in the RDS Rio Negro. Based on the distribution of other WSE hylids (Carvalho et al., 2018; Ferrão et al., 2019), we expect the new species to have a considerably wider distribution throughout WSEs in the Negro-Solimões Interfluve. Moreover, the surprisingly low genetic divergence (K2P and p-distances = 1.4%) between *S. albertinae* and *Scinax* sp. clade 72 from Guyana and Suriname (Vacher et al., 2020) indicates the possible occurrence of the new species in the Guiana Shield. We were not able to examine the Guyana and Suriname individuals morphologically, but if future analyses bolster our tentative conclusion that they are conspecific with *S. albertinae,* we hypothesize that ancestral populations of the new species and *Scinax* sp. clade 72 might have inhabited the eastern slopes of the Andes (where the sister species *S. wandae* currently occurs) and then split toward their current range. An alternate hypothesis is that emergence of the Negro River was a vicariant event responsible for limiting gene flow between northern and southern populations. Regardless of which of these hypotheses proves most likely, testing them requires a robust phylogeographic approach as well as an extensive sampling over intervening regions among target taxa.

According to our phylogenetic analyses, *Scinax albertinae* clusters with *S. cruentomma, S. wandae, S. strussmannae* and several undescribed species in a well-defined, monophyletic clade. This clade, together with its sister clade containing *S. fuscomarginatus, S. madeirae, S. villasboasi*, *S. parkeri* (Gaige, 1929) and *S. staufferi* (Cope, 1865), constitutes a well-supported, major clade of *Scinax* (Fig. 2, Appendix 3). Delimitation, structure and content of this large clade correspond well to earlier results by Ferrão et al. (2016) and Ferrão et al. (2018b).

By combining characters from morphology, karyology, and reproductive biology, Faivo-

vich (2002) evaluated the monophyly of *Scinax* species groups proposed by Fouquette and Delahoussaye (1977) and Duellman and Wiens (1992). He found that the *S. staufferi* species group as previously defined is polyphyletic, but at the same time he recovered a monophyletic *S. staufferi* clade containing *S. cruentomma, S. fuscomarginatus, S. nasicus, S. squalirostis, S. staufferi* and an undescribed species, *Scinax* sp. 2 (*S. nasicus* and *S. squalirostis* assume a different topology in Ferrão et al. [2018b] and in the present study). Within his *S. staufferi* clade, Faivovich (2002) recovered a minor clade composed of *S. cruentomma, S. fuscomarginatus,* and *S.* sp. 2, which is supported by two morphological synapomorphies: larynx strongly rotated in relation to the posteromedial processes, and subcylindrical cardiac process of the cricoid ring slightly wider than adjacent parts of the ring. These characters need to be assessed in other members of the major clade containing those species evidenced in the present study. Faivovich (2002) also noted that *S. cruentomma* and *S. fuscomarginatus* have a similar vocalization. Later, Carvalho et al. (2017) reported that the advertisement call of *S. exiguus* shares structural similarities with that of *S. fuscomarginatus*. The same structural pattern is observed herein in the advertisement calls of *S. albertinae, S. cruentomma, S. madeirae, S. staufferi, S. strussmannae, S. wandae, S. trilineatus* (Hoogmoed and Gorzula, 1979) and *S. parkeri* (Fig. 13). Indeed, the latter two species were recently synonymized with *S. fuscomarginatus* (Brusquetti et al., 2014). In light of these findings, reevaluation of the monophyly of the *S. staufferi* species group and its possible redefinition appear warranted.

ACKNOWLEDGMENTS

We dedicate this study to the memory of Dona Lúcia Toga, who always kindly supported research in the PPBio sampling module at the RDS Rio Negro. This study was funded by the Programa de Apoio aos Núcleos de Excelência (PRONEX) of the National Council for Scientific and Technological Development (CNPq) and Fundação de Amparo à Pesquisa do Estado do Amazonas (FAPEAM; Proj. 003/2009, Proc. 653/2009); the Museum of Comparative Zoology [MCZ] and David Rockfeller Center for Latin American Studies [DRCLAS], Harvard University; the Czech Republic Ministry of Culture (DKRVO 2019-2023/6.VI.d, National Museum Prague, 00023272); and Centro de Estudos Integrados da Biodiversidade Amazônica (CENBAM). We thank Ariane Silva (INPA-H), Andrés Rymel Acosta-Galvis (IAVH), Fernanda Werneck (INPA-H), José Rosado (MCZ), Michael Franzen (ZSM), and Santiago Ron (QCAZ) for granting access to specimens under their care; to BIOWEB Ecuador, Pontificia Universidad Católica del Ecuador (PUCE), Santiago Ron, and the QCAZ staff for making public data of specimens housed at QCAZ; to A. R. Acosta-Galvis, Igor Y. Fernandes, Rafael de Fraga and S. Ron for sharing photographs of *Scinax*; to Domingos J. Rodrigues, Marcos Penhacek and Samuel Anjos for sharing the vocalization of *S.* aff. *cruentomma*; and to Igor Y. Fernandes, Jussara Dayrell, and Rafaela Pereira for assistance with sampling. Miquéias Ferrão received a fellowship from CNPq (PDJ process 154325/2018-0), an Edward O. Wilson Biodiversity Postdoctoral Fellowship from the Harvard Museum of Comparative Zoology, and a fellowship from the David Rockefeller Center for Latin American Studies of Harvard University. Specimens were collected under IBAMA/ICMBio/RAN permits (02001.000508/2008-99; 1337-1). Protocols for animal collection and care followed the Conselho Federal de Biologia resolution 148/2012.

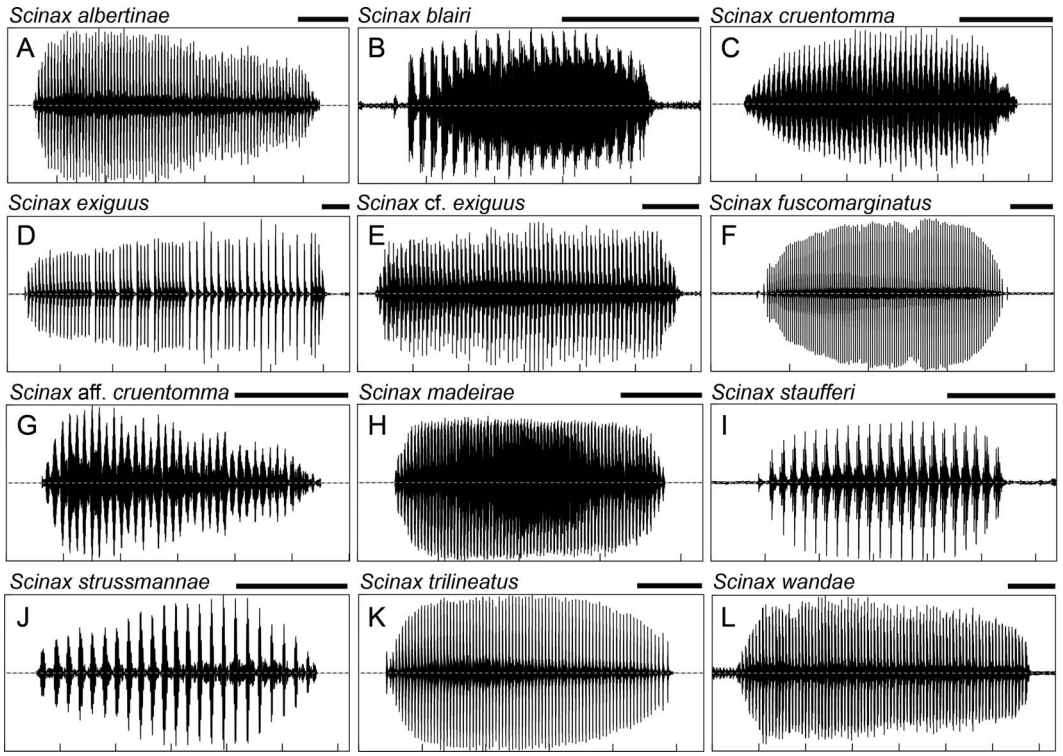

Figure 13. Advertisement calls of *Scinax albertinae* sp. nov. and close relatives. Call vouchers and localities: (A) FNJV50546, Rio Negro Sustainable Development Reserve, Novo Airão, Amazonas, Brazil. (B) ML218321, near junction of Ariari and Guaviare rivers, Vaupés, Colombia. (C) AM1TRC_AAGm671, Cucuí, São Gabriel da Cachoeira, Amazonas, Brazil. (D) ML194693, km 144 of the El Dorado–Sta. Elena de Uairén Road, Bolívar, Venezuela. (E) FNJV50555, Paiva Falls, Tepequém, Roraima, Brazil. (F) ML194674, Belém, Pará, Brazil. (G) Unvouchered, Juruena River, Cotriguaçu, Mato Grosso, Brazil. (H) ML196980, El Porvenir, Beni, Bolivia. (I) ML210707, Cordoba, Veracruz, Mexico. (J) Unvouchered, Nascentes do Lago Jari National Park, Tapauá, Amazonas, Brazil. (K) FNJV50554, Cantá, Roraima, Brazil. (L) BSA15980, San Martín, vereda Montebello, finca Tocancip, Meta, Colombia. Scale bars = 100 ms (A–I, K–L) and 40 ms (J).

Appendix 1. Specimens of *Scinax* and closely related taxa included in molecular analyses, with respective voucher numbers, localities, and GenBank accession numbers. Sequences of the new species are highlighted in bold. Asterisks denote samples shown in Figure 2.

Taxon	Voucher	Locality	GenBank
Julianus pinimus	CFBH 5788	Brazil, Rio Grande do Sul, Cambará do Sul	AY843681
Julianus pinimus	CFBHT 321	Brazil, Rio Grande do Sul, Cambará do Sul	KU495568
Julianus pinimus	CFBHT 11209	Brazil, Paraná, General Carneiro	KU495570
Julianus pinimus	CFBHT 11465	Brazil, Santa Catarina, Campos Novos	KU495569
Ololygon berthae	IIBPH 1396	Paraguay, Alto Vera, Itapua	KJ004191
Ololygon catharinae	MCP 3734	Brazil, Rio Grande Do Sul, Pro-Mata	AY843756
Ololygon faivovichi	MNRJ 40902	Brazil, São Paulo, Porcos Pequena	JN100002
Ololygon peixotoi	CFBH 9438	Brazil, São Paulo, Queimada Grande	JN100004
Ololygon perpusilla	CAB 1407	Brazil, São Paulo, Mar Virado	JN100001
Scinax acuminatus	IIBPH 277	Paraguay, Estancia San Jose, Neembucu	KJ004189
Scinax alter	CFBHT 03712	Brazil, Espírito Santo, Mimoso do Sul	KU495537
Scinax alter	MNRJ 38384	Brazil, Espirito Santo, Santa Teresa	MK266759
Scinax alter	MTR 12151	Brazil, Espírito Santo, Linhares, Reserva Vale do Rio Doce	KDQF01003196
Scinax boesemani	MTR 13736	Brazil, Amapá, Serra do Navio	KDQF01003247
Scinax boesemani	MTR 13975	Brazil, Amapá, Laranjal do Jari	KDQF01003304
Scinax boulengeri	MVZ 207215	Costa Rica, Guanacaste	AY843755
Scinax cf. *kennedyi*	AJC 1747	Colombia, Caserio Miraflores, Vereda La Balastrera, Almendros	KP149308
Scinax cf. *rostratus*	MTR 20499	Brazil, Roraima, Estação Ecológica Maracá, estrada lavrado	KDQF01003466
Scinax chiquitanus	HJ 598	Brazil, Amazonas, UHE Jirau, Mutum	KDQF01002665
Scinax chiquitanus	MJ 1314	Bolivia, Sara, Buenavista	JF789945
Scinax elaeochroa	MVZ 203919	Costa Rica, Limon	AY843755
Scinax elaeochroa	—	Costa Rica	EF376076
Scinax eurydice	MTR 05927	Brazil, Bahia, Serra do Teimoso, Jussari	KDQF01003135
Scinax eurydice	MTR 12172	Brazil, Espírito Santo, Linhares, FLONA Goytacazes	KDQF01003197
Scinax funereus	QCAZ 39444	Ecuador, Provincia Pastaza, Conambo, Bataburo Lodge	MH662480
Scinax funereus	QCAZ 43799	Ecuador, Provincia Orellana, El Descanso, Rio Napo	MH662481
Scinax fuscomarginatus	CFBH 10049	Brazil, São Paulo, Parque Estadual Morro do Diabo	KJ004110
Scinax fuscomarginatus	CFBH 14335	Brazil, Mato Grosso, Dom Aquino	KJ004176
Scinax fuscomarginatus	CFBH 18678	Brazil, São Paulo, Parque Estadual Morro do Diabo	KJ004111
Scinax fuscomarginatus	CFBH 21857	Brazil, Mato Grosso, Estação Ecológica Serra das Araras	KJ004177
Scinax fuscomarginatus	CFBH 24360	Brazil, Minas Gerais, Lagoa Santa	KJ004134
Scinax fuscomarginatus	CFBH 24361	Brazil, Minas Gerais, Lagoa Santa	KJ004135
Scinax fuscomarginatus	CHUNB 38023	Brazil, Tocantins, Paraná	KJ004122
Scinax fuscomarginatus	CHUNB 51003	Brazil, Bahia, Luis Eduardo Magalhães	KJ004123
Scinax fuscomarginatus	CHUNB 51004	Brazil, Bahia, São Desidério	KJ004124
Scinax fuscovarius	AF 384	Brazil, Minas Gerais, Lagoa Santa	KDQF01001465
Scinax fuscovarius	AS 0398	Bolivia, Nuflo de Chavez, San Sebastian	JF790013
Scinax garbei	WED 57696	Peru, Cusco Amazonico	DQ283030

Appendix 1. Continued.

Taxon	Voucher	Locality	GenBank
Scinax garbei	MPEG 33365	Brazil, Pará, APA Tapajós, Projeto Tocantizinho	KDQF01002963
Scinax garbei	QCAZ 46403	Ecuador, Provincia Morona Santiago, Napimias	MH662482
Scinax ictericus	CI 070	Peru, Los Amigos Biological Station, Manu, Madre de Dios	MN172527
Scinax imbegue	CFBHT 05890	Brazil, São Paulo, Peruíbe	KU495538
Scinax imbegue	CFBHT 19417	Brazil, São Paulo, Peruíbe, Estação Ecológica de Juréia Itatins	MH206262
Scinax iquitorum	NMP6V 71267/1	Peru, Puerto Almendras	KU317397
Scinax iquitorum	NMP6V 71267/3	Peru, Puerto Almendras	KU317398
Scinax jolyi	AF 0745	French Guiana, St Georges, savane	KDQF01000233
Scinax madeirae	CFBH 25469	Brazil, Rondônia, Porto Velho	KJ004101
Scinax madeirae	MNKA 9353	Bolivia, Los Lagos, Beni	KJ004100
Scinax nasicus	IIBPH 262	Paraguay, Neembucu Estancia San Jose	KJ004188
Scinax nasicus	MACN 38650	Argentina, Buenos Aires, Baradero, Estancia El retono	AY843759
Scinax nebulosus	AS 0148	Bolivia, Nuflo de Chavez, San Sebastian	JF790035
Scinax nebulosus	CFBHT 10951	Brazil, Piauí, Baixa Grande	KJ004190
Scinax nebulosus	LAJ 104	Brazil, Tocantins, UHE Lajeado	KDQF01002717
Scinax nebulosus	MTD 47705	Guyana, Iwokrama	KDQF01003029
Scinax nebulosus	MTR 13838	Brazil, Amapá, Serra do Navio	KDQF01003275
Scinax nebulosus	MTR 25655	Brazil, Rondônia, PARNA Pacaás Novos	KDQF01003626
Scinax onca	HJ 438	Brazil, Amazonas, UHE Jirau, Abunã	KDQF01002654
Scinax onca	HJ 661	Brazil, Amazonas, UHE Jirau, Abunã	KDQF01002673
Scinax onca	INPA-H 34586	Brazil, Amazonas, BR-319, RAPELD M7	KU317425
Scinax onca	INPA-H 34595	Brazil, Rondônia, Porto Velho, RAPELD M13	KU317419
Scinax parkeri	MJ 1289	Bolivia, nuflo de Chavez, San Sebastian	JF790005
Scinax parkeri	MJ 1316	Bolivia, Sara, Buenavista	JF790006
Scinax parkeri	INPA-H 34672	Brazil, Amazonas, BR-319, RAPELD M11	KU317410
Scinax parkeri	INPA-H 34676	Brazil, Amazonas, BR-319, RAPELD M11	KU317414
Scinax proboscideus	AF 0859	French Guiana, Chutes gregoire	KDQF01000285
Scinax rostratus	AJC 3506	Colombia, San Vicente de Chucuri, Vereda las Margaritas	KP149435
Scinax rostratus	CM 247	Venezuela, Rio Caura	EF376071
Scinax ruber	AJC 3532	Colombia, Santander, San Vicente de Chucuri	KP149347
Scinax ruber	AJC 3534	Colombia, Santander, San Vicente de Chucuri	KP149295
Scinax ruber	AJC 3936	Colombia, Miraflores, Vereda La Balastrera, Finca Los Almendros	KP149294
Scinax ruber	AJC 3940	Colombia, Miraflores, Vereda La Balastrera, Finca Los Almendros	KP149320
Scinax ruber	MPEG 30485	Brazil, Pará, FLOTA	KDQF01002917
Scinax ruber	MTD 48119	Suriname, Paramaribo	KDQF01003089
Scinax ruber	QCAZ 18217	Ecuador, Estacion Biologica Jatun Sacha	EF217487
Scinax ruber	AF 651	Brazil, Espírito Santo, UHE Rosal	KDQF01001480
Scinax ruber	AJC 2324	Colombia, Casanare, Municipio Orucue	KP149491
Scinax ruber	AJC 3884	Colombia, Santander, Sabana de Torres	KP149330
Scinax ruberoculatus	INPA-H 34610	Brazil, Rondônia, Porto Velho, RAPELD M8	KU317407
Scinax ruberoculatus	INPA-H 34705	Brazil, Rondônia, Porto Velho, RAPELD M9	KU317408
Scinax aff. *ruberoculatus*	AF 2089	Suriname, Sipaliwini, camp1 to Apalagadi	KDQF01000828

Appendix 1. Continued.

Taxon	Voucher	Locality	GenBank
Scinax aff. *ruberoculatus*	AF 2538	Suriname, Nassau	KDQF01000980
Scinax aff. *ruberoculatus*	CM 312	French Guiana, Kaw	KDQF01002287
Scinax aff. *ruberoculatus*	CM 316	French Guiana, Montsinery	KDQF01002290
Scinax sp. 2	—	Colombia, Llanos	EF217512
Scinax squalirostris	CFBH 21975	Brazil, Serra da Bocaina, Sao Paulo	KJ004187
Scinax squalirostris	CFBHT 10334	Brazil, São Paulo, São José do Barreiro	KU495564
Scinax squalirostris	CFBHT 00502	Brazil, São Paulo, Itirapina	KU495567
Scinax squalirostris	CFBHT 15638	Brazil, São Paulo, São José do Barreiro, Serra da Bocaina	KU495565
Scinax squalirostris	CFBHT 01415	Brazil, Minas Gerais, São Roque de Minas	KU495563
Scinax squalirostris	CFBHT 08180	Brazil, Rio Grande do Sul, Bom Jesus	KU495566
Scinax staufferi	UTAA 50749	Guatemala, Zacapa, 2.9 km S Teculutan	AY843761
Scinax trilineatus	AF 2142	Suriname, Sipaliwini	KDQF01000859
Scinax trilineatus	CFBH 29521	Brazil, Roraima, Boa Vista	KJ004121
Scinax tymbamirim	CFBHT 21497	Brazil, São Paulo, São Sebastião, Parque Estadual Serra do Mar	MH206342
Scinax tymbamirim	CFBHT 21498	Brazil, São Paulo, São Sebastião, Parque Estadual Serra do Mar	MH206343
Scinax villasboasi	CHUNB 34502	Brazil, Pará, Serra do Cachimbo	KJ004103
Scinax villasboasi	CHUNB 34503	Brazil, Pará, Serra do Cachimbo	KJ004104
Scinax x-signatus	MTJ 0578	Brazil, Minas Gerais, Parque Nacional Cavernas do Peruacu	KDQF01003120
Scinax x-signatus	MTR 13988	Brazil, Amapá, Macapá	KDQF01003307
* *Scinax albertinae* sp. nov.	INPA-H 42867	Brazil, Amazonas, Novo Airão, RDS Rio Negro	**MW853693**
* *Scinax albertinae* sp. nov.	INPA-H 42869	Brazil, Amazonas, Novo Airão, RDS Rio Negro	**MW853694**
* *Scinax albertinae* sp. nov.	INPA-H 42863	Brazil, Amazonas, Novo Airão, RDS Rio Negro	**MW853695**
* *Scinax albertinae* sp. nov.	INPA-H 42864	Brazil, Amazonas, Novo Airão, RDS Rio Negro	**MW853696**
* *Scinax cruentomma* clade 49	INPA-H 34697	Brazil, Amazonas, BR-319, RAPELD M1	KU317385
* *Scinax cruentomma* clade 49	MTR 18678	Brazil, Amazonas, Rio Purus	KDQF01003383
* *Scinax cruentomma* clade 49	MTR 18934	Brazil, Amazonas, Rio Purus, Lago Chaviana, Itapuru, right bank	KDQF01003409
* *Scinax cruentomma* clade 49	MTR 19192	Brazil, Amazonas, Rio Purus, Moiobamba, right bank	KDQF01003426
* *Scinax* aff. *cruentomma*	INPA-H 34596	Brazil, Amazonas, BR-319, RAPELD M6	KU317386
* *Scinax* aff. *exiguus* clade 50	MTR 20573	Brazil, Roraima, Estação Ecológica Maracá, trilha lateral aterro	KDQF01003479
* *Scinax* aff. *exiguus* clade 50	MTR 20813	Brazil, Roraima, Pacaraima, Marco BV8	KDQF01003512
* *Scinax strussmannae*	INPA-H 34688	Brazil, Amazonas, BR-319, RAPELD M9	KU317428
* *Scinax strussmannae*	INPA-H 34690	Brazil, Amazonas, BR-319, RAPELD M9	KU317431
* *Scinax strussmannae*	INPA-H 34700	Brazil, Amazonas, BR-319, RAPELD M9	KU317430
* *Scinax wandae* clade 46	ANDES-A 1072	Colombia, Casanare, Sabanalarga, Sabanalarga	KP149323
* *Scinax wandae* clade 46	ANDES-A 1077	Colombia, Casanare, Sabanalarga, Sabanalarga	KP149381
* *Scinax wandae* clade 46	ANDES-A 1234	Colombia, Casanare, Sabanalarga, Sabanalarga	KP149319
* *Scinax* sp. 4	INPA-H 34693	Brazil, Amazonas, BR-319, RAPELD M11	KU317429
* *Scinax* sp. 6 clade 48	INPA-H 34597	Brazil, Amazonas, Careiro, RAPELD M1	KU317391

Appendix 1. Continued.

Taxon	Voucher	Locality	GenBank
* *Scinax* sp. 6 clade 48	INPA-H 35561	Brazil, Rondônia, Porto Velho, RAPELD M18	KU317392
* *Scinax* sp. 6 clade 48	INPA-H 35563	Brazil, Rondônia, Porto Velho, RAPELD M13	KU317393
* *Scinax* sp. 6 clade 48	INPA-H 35564	Brazil, Rondônia, Porto Velho, RAPELD M17	KU317389
* *Scinax* sp. 6 clade 48	INPA-H 35565	Brazil, Rondônia, Porto Velho, RAPELD M17	KU317390
* *Scinax* sp. 6 clade 48	INPA-H 35567	Brazil, Rondônia, Porto Velho, RAPELD M17	KU317396
* *Scinax* sp. 6 clade 48	HJ 425	Brazil, Amazonas, UHE Jirau, Abunã	KDQF01002652
* *Scinax* sp. 6 clade 48	MTR 19225	Brazil, Amazonas, Rio Purus	KDQF01003430
* *Scinax* sp. clade 45	AG 073	French Guiana, Trinite, Crique Grand Leblond	EF217491
* *Scinax* sp. clade 45	AG 198	French Guiana, Trinite, Crique Grand Leblond	EF217493
* *Scinax* sp. clade 45	CAAM 32	French Guiana, Montagne Cacao	KDQF01002143
* *Scinax* sp. clade 45	CM 255	French Guiana, Aratai	EF217495
* *Scinax* sp. clade 45	CM 256	French Guiana, Aratai	EF217494
* *Scinax* sp. clade 45	CM 257	French Guiana, Aratai	EF217492
* *Scinax* sp. clade 47	AF 2405	Suriname, Nassau, Trail 7	KDQF01000941
* *Scinax* sp. clade 47	AG 421	French Guiana, Atachi Bakka	KDQF01001592
* *Scinax* sp. clade 47	MTD 48006	Guyana, Iwokrama	KDQF01003085
* *Scinax* sp. clade 62	AJC 1743	Colombia, Meta, San Juan de Arama	KP149376
* *Scinax* sp. clade 62	AJC 3464	Colombia, Meta, San Juan de Arama	KP149460
* *Scinax* sp. clade 62	AJC 3461	Colombia, Meta, San Juan de Arama	KP149431
* *Scinax* sp. clade 62	AJC 3942	Colombia, Meta, San Juan de Arama	KP149372
* *Scinax* sp. clade 71	MTR 13734	Brazil, Amapá, Serra do Navio	KDQF01003246
* *Scinax* sp. clade 71	MTR 13778	Brazil, Amapá, Serra do Navio	KDQF01003261
* *Scinax* sp. clade 72	BPN 1100	Suriname, Sipaliwini	KDQF01001958
* *Scinax* sp. clade 72	BPN 1167	Guyana, Imbaimadai	KDQF01001965
* *Scinax* sp. clade 72	BPN 1168	Guyana, Imbaimadai	KDQF01001966
Sphaenorhynchus surdus	CFBHT 05536	Brazil, Santa Catarina, Lebon Regis	KU495592

Appendix 2. Specimens examined. ***Hyla affinis***: BRAZIL: "fluminis Amazonum" = Rio Amazonas (ZSM 2495/0 [holotype, photo]). ***Scinax baumgardneri***: VENEZUELA: Amazonas: (MCZ-A 28563 [holotype]). ***Scinax blairi***: COLOMBIA: Vaupes, near junction of Rio Guaviare and Rio Ariari (MCZ-A 81819 [paratype]). ***Scinax boesemani***: SURINAME: Paramaribo: near Zanderij (RMNH 12601 [holotype, photo], MCZ-A 52833 [paratype]). BRAZIL: Roraima: Caracaraí, Viruá National Park (INPA-H 25972, 25974). ***Scinax chiquitanus***: BRAZIL: Rondônia: Porto Velho (INPA-H 35554–58, 35560). ***Scinax cruentomma***: ECUADOR: Napo: Santa Cecilia (KU 126587 [holotype, photo]); Orellana: Parque Nacional Yasuní (QCAZ-A 8184), Río Napo (QCAZ-A 43772, 44754). BRAZIL: Amazonas: Careiro da Várzea, Ramal do Purupuru (INPA-H 34697). ***Scinax funereus***: ECUADOR: Orellana: Río Napo, Primavera (QCAZ-A 43799, photo), Tambococha (QCAZ-A 55280, 55283; photo); Napo: Limoncocha (MCZ-A 97672). ***Scinax fuscomarginatus***: BRAZIL: Roraima: Boa Vista, Maracá Ecological Station (INPA-H 34634, 34646, 34661–62); Caracaraí, Viruá National Park (INPA-H 19371–72, 19376, 19378, 19383–84). ***Scinax garbei***: BRAZIL: Roraima: Caracaraí, Viruá National Park (INPA-H 25964, 27496). ECUADOR: Napo: Limoncocha (MCZ-A 97672). ***Scinax madeirae***: BRAZIL: Rondônia: Alta Floresta, Corumbiaria Park (INPA-H 7050–51); Porto Velho (MCZ-A 64371 [paratype]). ***Scinax nebulosus***: BRAZIL: Pará: Alter do Chão (INPA-H 34647, 34653); Rondônia: Costa Marques, Real Forte Príncipe da Beira (INPA-H 34641); Roraima: Caracaraí, Parque Nacional do Viruá (INPA-H 27535–37). ***Scinax onca***: BRAZIL: Amazonas: Beruri (INPA-H 34584 [holotype], 20582, 20585–86 34581, 34583, 34587 [praatypes]); Rondônia: Porto Velho (INPA-H 34588–95 [paratypes]). ***Scinax proboscideus***: BRAZIL: Amazonas: Manaus, Colosso Reserve at PDBFF (INPA-H 10304); Presidente Figueiredo, Vila Pitinga (INPA-H 1870); Pará: Oriximiná (INPA-H 304). ***Scinax ruberoculatus***: BRAZIL: Amazonas: Careiro da Várzea, BR-319, km 100 (INPA-H 34598, 34600–01, 34604, 34614–15, 34622, 34624, 34627, 34629 [paratypes]), km 168 (INPA-H 34602 [paratype]); Borba, BR-319, km 220 (INPA-H

34610, 34620 [paratypes]); Beruri, BR-319, km 220 (INPA-H 34608 [paratype]), km 360 (INPA-H 34599, 34607, 34609, 34611–12, 34617–18, 34621, 34625–26, 34628, 34630 [paratypes]); Manicoré, BR-319, km 400 (INPA-H 34603, 34606, 34616, 34623 [paratypes]); Tapauá, BR-319 km 450, Nascentes do Lago Jari National Park (INPA-H 34665 [holotype], 34605, 34613, 34619 [paratypes]). ***Scinax squalirostris***: URUGUAY: 15 km northeast of San Carlos, Alvarez Farm (MCZ-A 25761 [holotype of *Hyla evelynae*]). ***Scinax strussmannae***: BRAZIL: Amazonas: Tapauá, Nascentes do Lago Jari National Park (INPA-H 34688 [holotype]; 34689–92, 34700 [paratypes]). ***Scinax wandae***: COLOMBIA: Meta: La Macarena (IAvH-Am 15107, 15256–59, 15263–64, 15276); Casarane: Sabanalarga (ANDES-A 1068, 1072, 1077, 1234).

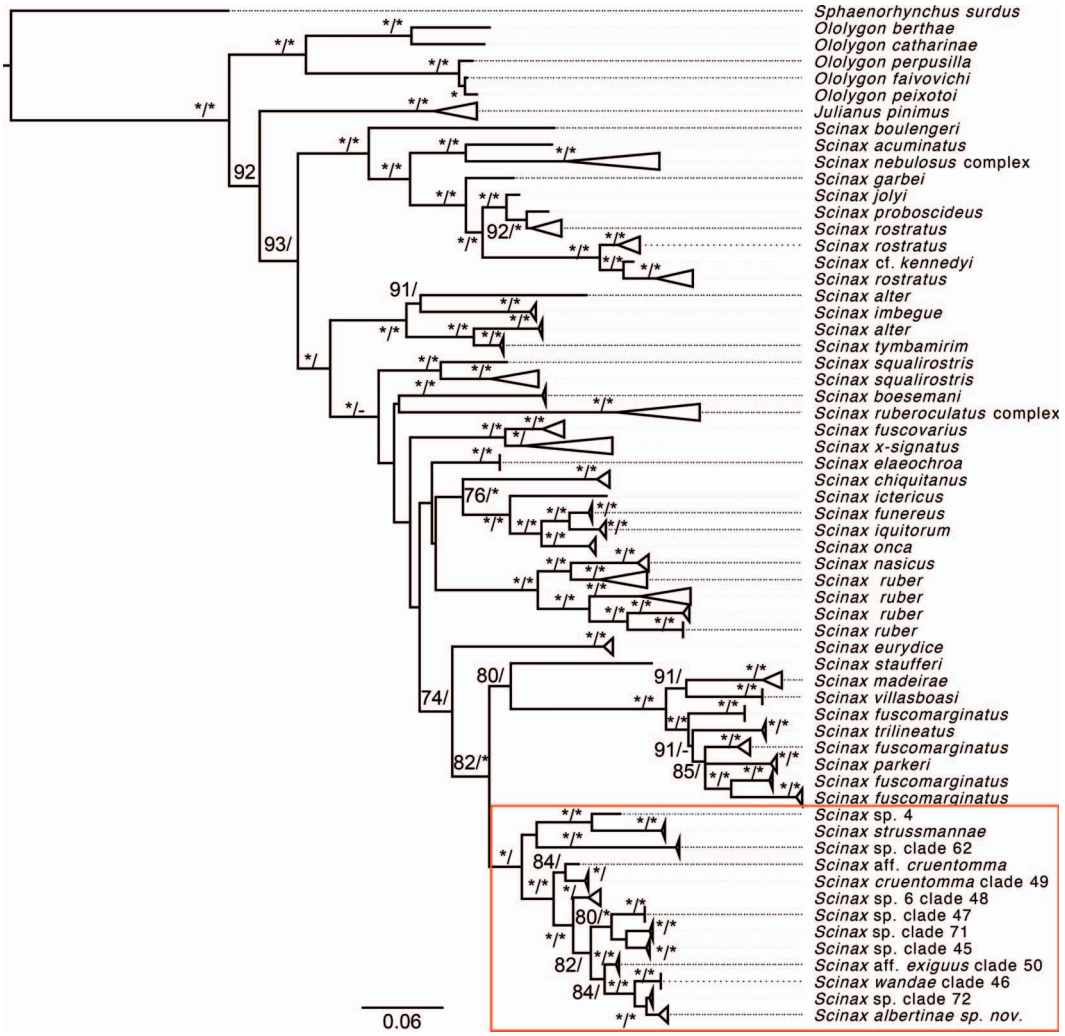

Appendix 3. Bayesian phylogenetic inference of *Scinax* diversification based on a fragment of the 16S rDNA mitochondrial gene, including sequences of the three most closely related genera *Julianus, Ololygon,* and *Sphaenorhynchus*. The red rectangle encloses the major clade where the new species is nested; that clade is fully expanded in Figure 2. Two support values are shown along each branch: bootstrap of a Maximum Likelihood analysis (before slash) and Bayesian posterior probability (after slash); values below 75 and 0.95 are omitted, above 95 and 0.95 are denoted by an asterisk.

LITERATURE CITED

Acosta-Galvis, A. R. 2018. Una nueva rana de huesos verdes del género *Scinax* (Anura: Hylidae) asociada a los bosques subandinos de la cuenca del río Magdalena, Colombia. *Biota Colombiana* 19: 131–159. [In Spanish.]

Adeney, J. M., N. Christensen, A. Vicentini, and M. Cohn-Haft. 2016. White-sand ecosystems in Amazonia. *Biotropica* 48: 7–23.

Ale-Rocha, R., and R. M. Vieira. 2008. Hybotinae (Diptera, Hybotidae) of the National Park of Jaú, Amazonas, Brazil, with description of five new species of *Syneches* Walker. *Acta Amazonica* 38: 113–126.

Almeida, R. A. M. 2016. Aves Linnaeus, 1758: new records for the Jaú National Park, Amazonas, Brazil. *Check List* 6: 495–498.

Altig, R., and R. W. McDiarmid. 1999. Body plan: development and morphology, Pp. 24–51 in: R. W. McDiarmid and R. Altig, editors. *Tadpoles: the biology of anuran larvae*. Chicago: University of Chicago Press.

Araujo-Vieira, K., B. L. Blotto, U. Caramaschi, C. F. B. Haddad, J. Faivovich, and T. Grant. 2019. A total evidence analysis of the phylogeny of hatchet-faced treefrogs (Anura: Hylidae: *Sphaenorhynchus*). *Cladistics* 35: 469–486.

Araujo-Vieira, K., J. P. Pombal, Jr., U. Caramaschi, G. Novaes-e-Fagundes, V. G. D. Orrico, and J. Faivovich. 2020. A neotype for *Hyla x-signata* Spix, 1824 (Amphibia, Anura, Hylidae). *Papéis Avulsos de Zoologia* 60: e20206056.

Bell, R. C., C. A. Brasileiro, C. F. B. Haddad, and K. R. Zamudio. 2012. Evolutionary history of *Scinax* treefrogs on land-bridge islands in south-eastern Brazil. *Journal of Biogeography* 39: 1733–1742.

Bioacoustics Research Program. 2014. Raven Pro: interactive sound analysis software. Version 1.5. Ithaca, New York: The Cornell Lab of Ornithology. [cited 2021 April 2]. Available from: http://www.birds.cornell.edu/brp/raven/RavenOverview.html.

Bokermann, W. C. A. 1964. Dos nuevas especies de *Hyla* de Rondonia, Brasil (Amphibia, Salientia, Hylidae). *Neotropica* 10: 3–6. [In Spanish.]

Borges, S. H., M. Cohn-Haft, A. M. P. Carvalhães, L. M. Henriques, J. F. Pacheco, and A. Whittaker. 2001. Birds of Jaú National Park, Brazilian Amazon: species check-list, biogeography and conservation. *Ornitologia Neotropical* 12: 109–140.

Borges, S. H., C. Cornelius, M. Moreira, C. C. Ribas, M. Conh-Haft, J. M. Capurucho, C. Vargas, and R. Almeida. 2016. Bird communities in Amazonian white-sand vegetation patches: effects of landscape configuration and biogeographic context. *Biotropica* 48: 121–131.

Brongersma, L. D. 1933. Ein neuer Laubfrosch aus Surinam. *Zoologischer Anzeiger* 103: 267–270. [In German.]

Brusquetti, F., M. Jansen, C. Barrio-Amarós, M. Segalla, and C. F. B. Haddad. 2014. Taxonomic review of *Scinax fuscomarginatus* (Lutz, 1925) and related species (Anura; Hylidae). *Zoological Journal of the Linnean Society* 171: 783–821.

Capurucho, J. M. G., C. Cornelius, S. H. Borges, M. Cohn-Haft, A. Aleixo, J. P. Metzger, and C. C. Ribas. 2013. Combining phylogeography and landscape genetics of *Xenopipo atronitens* (Aves: Pipridae), a white sand campina specialist, to understand Pleistocene landscape evolution in Amazonia. *Biological Journal of the Linnean Society* 110: 60–76.

Carvalho, T. R., P. Azarak, D. Bang, W. E. Duellman, and A. A. Giaretta. 2017. A reassessment of the vocalization and distribution of *Scinax exiguus* (Duellman, 1986) (Anura: Hylidae) in the Amazonian savanna of Roraima, northern Brazil, with the description of its aggressive call. *Neotropical Biodiversity* 3: 196–202.

Carvalho, T. R., B. F. V. Teixeira, W. E. Duellman, and A. A. Giaretta. 2015. *Scinax cruentommus* (Anura: Hylidae) in the upper Rio Negro drainage, Amazonas state, Brazil, with the redescription of its advertisement call. *Phyllomedusa* 14: 139–146.

Carvalho, V. T., R. de Fraga, S. Bittencourt, L. Bonora, L. H. Condrati, M. Gordo, and R. C. Vogt. 2018. Geographic distribution of *Aparasphenodon venezolanus* (Anura: Hylidae) in the Brazilian Amazon lowlands. *Phyllomedusa* 17: 139–144.

Cochran, D. M. 1953. Three new Brazilian frogs. *Herpetologica* 8: 111–115.

Cohn-Haft, M., M. A. Santos, Jr., A. M. Fernandes, and C. C. Ribas. 2013. A new species of *Cyanocorax* jay from savannas of the central Amazon, Pp. 306–310 in: J. del Hoyo, A. Elliott, J. Sargatal, and D. Christie, editors. *Handbook of the Birds of the World. Special volume. New Species and Global Index*. Barcelona: Lynx Edicions.

Cope, E. D. 1865. Third contribution to the herpetology of tropical America. *Proceedings of the Academy of Natural Sciences of Philadelphia* 17: 185–198.

Cope, E. D. 1874. On some Batrachia and Nematognathi brought from the upper Amazon by Prof. Orton. *Proceedings of the Academy of Natural Sciences of Philadelphia* 26: 120–137.

Costa, F. M., M. H. Terra-Araujo, C. E. Zartman, C. Cornelius, F. A. Carvalho, M. J. G. Hopkins, P. L.

Viana, E. M. B. Prata, and A. Vicentini. 2020. Islands in a green ocean: spatially structured endemism in Amazonian white-sand vegetation. *Biotropica* 52: 34–45.

De la Riva, I. 1990. Una especie nueva de *Ololygon* (Anura: Hylidae) procedente de Bolivia. *Revista Española de Herpetología* 4: 81–86. [In Spanish.]

Duellman, W. E. 1970. The hylid frogs of Middle America. *Monograph of the Museum of Natural History, University of Kansas* 1: 1–428.

Duellman, W. E. 1971. The identities of some Ecuadorian hylid frogs. *Herpetologica* 27: 212–227.

Duellman, W. E. 1972a. South American frogs of the *Hyla rostrata* group (Amphibia, Anura, Hylidae). *Zoologische Mededelingen* 47: 177–192.

Duellman, W. E. 1972b. A new species of *Hyla* from Amazonian Ecuador. *Copeia* 1972: 265–271.

Duellman, W. E. 1986. Two new species of *Ololygon* (Anura: Hylidae) from the Venezuelan Guyana. *Copeia* 1986: 864–870.

Duellman, W. E., and J. J. Wiens. 1992. The status of the hylid frog genus *Ololygon* and the recognition of *Scinax* Wagler, 1830. *Occasional Papers of the Museum of Natural History, University of Kansas* 151: 1–23.

Duellman, W. E., and J. J. Wiens. 1993. Hylid frogs of the genus *Scinax* Wagler, 1830, in Amazonian Ecuador and Peru. *Occasional Papers of the Museum of Natural History, University of Kansas* 153: 1–57.

Eiten, G. 1978. Delimitation of the Cerrado concept. *Vegetatio* 36: 169–178.

Faivovich, J. 2002. A cladistic analysis of *Scinax* (Anura: Hylidae). *Cladistics* 18: 367–393.

Faivovich, J., C. F. B. Haddad, P. C. A. Garcia, D. R. Frost, J. A. Campbell, and W. C. Wheeler. 2005. Systematic review of the frog family Hylidae, with special reference to Hylinae: phylogenetic analysis and taxonomic revision. *Bulletin of the American Museum of Natural History* 294: 1–240.

Ferrão, M., O. Colatreli, R. de Fraga, I. L. Kaefer, J. Moravec, and A. P. Lima. 2016. High species richness of *Scinax* treefrogs (Hylidae) in a threatened Amazonian landscape revealed by an integrative approach. *PLoS ONE* 11: e0165679.

Ferrão, M., R. de Fraga, J. Moravec, I. L. Kaefer, and A. P. Lima. 2018a. A new species of Amazonian snouted treefrog (Hylidae: *Scinax*) with description of a novel species-habitat association for an aquatic breeding frog. *PeerJ* 6: 4321.

Ferrão, M., J. Moravec, R. de Fraga, A. P. Almeida, I. L. Kaefer, and A. P. Lima. 2017. A new species of *Scinax* from the Purus–Madeira interfluve, Brazilian Amazonia (Anura, Hylidae). *ZooKeys* 706: 137–162.

Ferrão, M., J. Moravec, I. L. Kaefer, R. de Fraga, and A. P. Lima. 2018b. New species of *Scinax* (Anura: Hylidae) with red-striped eyes from Brazilian Amazonia. *Journal of Herpetology* 52: 473–486.

Ferrão, M., J. Moravec, L. J. C. L. Moraes, V. T. Carvalho, M. Gordo, and A. P. Lima. 2019. Rediscovery of *Osteocephalus vilarsi* (Anura: Hylidae): an overlooked but widespread Amazonian spiny-backed treefrog. *PeerJ* 7: e8160.

Ferreira, A. S., J. Moravec, M. Ferrão, and A. P. Lima. 2019. Association of *Hemidactylus palaichthus* Kluge, 1969 (Squamata, Gekkonidae) with the bromeliad *Aechmea huebneri*. *North-Western Journal of Zoology* 15: 188–191.

Fine, P. V. A., and C. Baraloto. 2016. Habitat endemism in white-sand forests: insights into the mechanisms of lineage diversification and community assembly of the Neotropical flora. *Biotropica* 48: 24–33.

Fitzinger, L. J. F. J. 1843. *Systema Reptilium. Fasciculus Primus*. Wien: Braumüller et Seidel.

Fouquet, A., M. Vences, M. D. Salducci, A. Meyer, C. Marty, and A. Gilles. 2007. Revealing cryptic diversity using molecular phylogenetics and phylogeography in frogs of the *Scinax ruber* and *Rhinella margaritifera* species groups. *Molecular Phylogenetics and Evolution* 43: 567–582.

Fouquette, M.J., Jr., and A.J. Delahoussaye. 1977. Sperm morphology in the *Hyla rubra* group (Amphibia, Anura, Hylidae), and its bearing on generic status. *Journal of Herpetology* 11: 387–396.

Fouquette, M. J., Jr., and W. F. Pyburn. 1972. A new Colombian treefrog of the *Hyla rubra* complex. *Herpetologica* 28: 176–181.

Fraga, R., E. Souza, A. P. Santos-Jr. and R. A. Kawashita-Ribeiro. 2018. Notes on the rare *Mastigodryas moratoi* (Serpentes: Colubridae) in the Brazilian Amazon white-sand forests. *Phyllomedusa* 17: 299–302.

Frost, D. R., T. Grant, J. Faivovich, R. H. Bain, A. Haas, C. F. B. Haddad, R. O. De Sá, A. Channing, M. Wilkinson, S. C. Donnellan, C. J. Raxworthy, J. A. Campbell, B. L. Blotto, P. Moler, R. C. Drewes, R. A. Nussbaum, J. D. Lynch, D. M. Green, and W. C. Wheeler. 2006. The amphibian tree of life. *Bulletin of the American Museum of Natural History* 297:1–370.

Gaem, P. H., F. Farroñay, F. F. Mazine, and A. Vicentini. 2019. *Myrcia psammophila* (Myrtaceae), a new species from the Amazonian white-sand vegetation. *Phytotaxa* 414: 253–261.

Gaige, H. T. 1929. Three new tree-frogs from Panama and Bolivia. *Occasional Papers of the Museum of Zoology, University of Michigan* 207: 1–6.

Goin, C. J. 1966. Description of a new frog of the genus *Hyla* from Suriname. *Zoologische Mededelingen* 41: 229–232.

Goldberg, J., D. Cardozo, F. Brusquetti, D. B. Villafañe, A. C. Gini, and C. Bianchi. 2018. Body size variation and sexual size dimorphism across climatic gradients in the widespread treefrog *Scinax fuscovarius* (Anura, Hylidae). *Austral Ecology* 43: 35–45.

Gordo, M., L. F. Toledo, P. Suárez, R. A. Kawashita-Ribeiro, R. W. Ávila, D. H. Morais, and I. Nunes. 2013. A new species of Milk Frog of the genus *Trachycephalus Tschudi* (Anura, Hylidae) from the Amazonian rainforest. *Herpetologica* 69: 466–479.

Gosner, K. L. 1960. A simplified table for staging anuran embryos and larvae with notes on identification. *Herpetologica* 16: 183–190.

Guarnizo, C. E., A. Paz, A. Muñoz-Ortiz, S. V. Flechas, J. Méndez-Narvaéz, and A. J. Crawford. 2015. DNA barcoding survey of anurans across the Eastern Cordillera of Colombia and the impact of the Andes on cryptic diversity. *PloS ONE* 10: e0127312.

Haas, A., and I. Das. 2011. Describing east Malaysian tadpole diversity: status and recommendations for standards and procedures associated with larval amphibian description and documentation. *Bonner Zoologische Monographien* 57: 29–46.

Hall, T. A. 1999. BioEdit: a user-friendly biological sequence alignment editor and analysis program for Windows 95/98/NT. *Nucleic Acids Symposium Series* 41: 95–98.

Henle, K. 1991. *Ololygon pedromedinae* sp. nov., ein neuer Knickzehenlaubfrosch (Hylidae) aus Peru. *Salamandra* 27: 76–82.

Heyer, W. R., A. S. Rand, C. A. G. Cruz, O. L. Peixoto, and C. E. Nelson. 1990. Frogs of Boracéia. *Arquivos de Zoologia* 31: 231–410.

Hoang, D. T., O. Chernomor, A. von Haeseler, B. Q. Minh, and L. S. Vinh. 2018. UFBoot2: improving the ultrafast bootstrap approximation. *Molecular Biology and Evolution* 35: 518–522.

Hoogmoed, M. S., and S. J. Gorzula. 1979. Checklist of the savanna inhabiting frogs of the El Manteco region with notes on their ecology and the description of a new species of treefrog (Hylidae, Anura). *Zoologische Mededelingen. Leiden* 54: 183–216.

Jansen, M., R. Bloch, A. Schulze, and M. Pfenninger. 2011. Integrative inventory of Bolivia's lowland anurans reveals hidden diversity. *Zoologica Scripta* 40: 567–583.

Katoh, K., and D. M. Standley. 2013. MAFFT Multiple sequence alignment software version 7: improvements in performance and usability. *Molecular Biology and Evolution* 30: 772–780.

Kimura, M. 1980. A simple method for estimating evolutionary rate of base substitutions through comparative studies of nucleotide sequences. *Journal of Molecular Evolution* 16: 111–120.

Kluge, A. G. 1969. The evolution and geographical origin of the New World *Hemidactylus mabouia-brooki* complex (Gekkonidae, Sauria). *Miscellaneous Publications, Museum of Zoology, University of Michigan* 138: 1–78.

Köhler, J., M. Jansen, A. Rodriguez, P. J. R. Kok, L. P. Toledo, M. Emmrich, F. Glaw, C. F. B. Haddad, M. O. Rödel, and M. Vences. 2017. The use of bioacoustics in anuran taxonomy: theory, terminology, methods and recommendations for best practice. *Zootaxa* 4251: 1–124.

Lamarre, G. P., D. S. Amoretti, C. Baraloto, F. Bénéluz, I. Mesones, and P. V. Fine. 2016. Phylogenetic overdispersion in Lepidoptera communities of Amazonian white-sand forests. *Biotropica* 48: 101–109.

Lanfear, R., P. B. Frandsen, A. M. Wright, T. Senfeld, and B. Calcott. 2017. PartitionFinder 2: new methods for selecting partitioned models of evolution for molecular and morphological phylogenetic analyses. *Molecular Biology and Evolution* 34: 772–773.

Laurenti, J. N. 1768. *Specimen Medicum, Exhibens Synopsin Reptilium Emendatum cum Experimentis Circa Venena et Antidota Reptilium Austriacorum*. Wien: Joan. Thom. nob. de Trattnern. [In Latin.]

Lescure, J., and C. Marty. 2000. Atlas des Amphibiens de Guyane. *Collections Patrimoines Naturels* 45: 1–388.

Lima, A. P., A. S. Ferreira, J. Dayrell, R. C. S. Pereira, W. E. Magnusson, and M. Ferrão. 2021. *Sapos da RDS Rio Negro. Região do Ramal do Uga-Uga*. Manaus: INPA.

Lopes, A. G., D. L. Bang, P. Marinho, and A. A. Giaretta. 2020. Acoustics suggests hidden diversity in *Scinax garbei* (Anura: Hylidae). *Phyllomedusa* 19: 63–82.

Lutz, A. 1925a. Batraciens du Brésil. *Comptes Rendus et Mémoires Hebdomadaires des Séances de la Société de Biologie et des ses Filiales. Paris* 93: 137–139. [In French.]

Lutz, A. 1925b. Batraciens du Brésil. *Comptes Rendus et Mémoires Hebdomadaires des Séances de la Société de Biologie et des ses Filiales. Paris* 93: 211–214. [In French.]

Lyra, M. L., C. F. B. Haddad, and A. M. L. Azeredo-Espin. 2017. Meeting the challenge of DNA barcoding Neotropical amphibians: polymerase

chain reaction optimization and new COI primers. *Molecular Ecology Resources* 17: 966–980.

Melin, D. E. 1941. Contributions to the knowledge of the Amphibia of South America. *Göteborgs Kungl. Vetenskaps-och Vitterhets-samhälles. Handlingar. Serien B, Matematiska och Naturvetenskapliga Skrifter* 1: 1–71.

Mertens, R. 1950. Ein neuer Laubfrosch aus Venezuela. *Senckenbergiana Biologica* 31: 1–10.

Miranda-Ribeiro, A. 1926. Notas para servirem ao estudo dos Gymnobatrachios (Anura) Brasileiros. *Arquivos do Museu Nacional* 27: 1–227. [In Portuguese.]

Moravec, J., I. A. Tuanama, P. E. Pérez-Peña, and E. Lehr. 2009. A new species of *Scinax* (Anura: Hylidae) from the area of Iquitos, Amazonian Peru. *South American Journal of Herpetology* 4: 9–16.

Myers, C. W., and W. E. Duellman. 1982. A new species of *Hyla* from Cerro Colorado, and other tree frog records and geographical notes from Western Panama. *American Museum Novitates* 2752: 1–32.

Napoli, M. F. 2005. A new species of allied to *Hyla circumdata* (Anura: Hylidae) from Serra da Mantiqueira, southeastern Brazil. *Herpetologica* 61: 63–69.

Nguyen, L. T., H. A. Schmidt, A. von Haeseler, and B. Q. Minh. 2015. IQ-TREE: a fast and effective stochastic algorithm for estimating Maximum-Likelihood phylogenies. *Molecular Biology and Evolution* 32: 268–274.

Palumbi, S. R. 1991. Nucleic acids II: the polymerase chain reaction, Pp. 205–47 in: D. M. Hillis, C. Moritz, and B. K. Mable, editors. *Molecular Systematics*. Sunderland, Massachusetts: Sinauer & Associates Inc.

Parker, H. W. 1940. Undescribed anatomical structures and new species of reptiles and amphibians. *Annals and Magazine of Natural History* 5: 257–274.

Peters, W. C. H. 1863. Fernere Mittheilungen über neue Batrachier. *Monatsberichte der Königlichen Preussischen Akademie der Wissenschaften zu Berlin* 1863: 445–470. [In German.]

Pyburn, W. F. 1992. A new tree frog of the genus *Scinax* from the Vaupes River of northwestern Brazil. *Texas Journal of Science* 44: 405–411.

Pyburn, W. F. 1993. A new species of dimorphic tree frog, genus *Hyla* (Amphibia: Anura: Hyldiae), from the Vaupés River of Colombia. *Proceedings of the Biological Society of Washington* 106: 46–50.

Pyburn, W. F., and M. J. Fouquette. 1971. A new striped treefrog from central Colombia. *Journal of Herpetology* 5: 97–101.

R Core Team. 2019. A language and environment for statistical computing. Vienna: R Foundation for Statistical Computing. [cited 2021 April 2]. Available from: http://www.r-project.org/.

Rambaut, A., A. J. Drummond, D. Xie, G. Baele, and M. A. Suchard. 2018. Posterior summarization in Bayesian phylogenetics using Tracer 1.7. *Systematic Biology* 67: 901–904.

Randrianiaina, R. D., A. Strauÿ, J. Glos, F. Glaw, and M. Vences. 2011. Diversity, external morphology and 'reverse taxonomy' in the specialized tadpoles of Malagasy river bank frogs of the subgenus *Ochthomantis* (genus *Mantidactylus*). *Contributions to Zoology* 80:17–65.

Rivero, J. A. 1961. Salientia of Venezuela. *Bulletin of the Museum of Comparative Zoology* 126: 1–207.

Rojas-Zamora, R. R., V. T. Carvalho, R. W. Ávila, I. P. Farias, M. Gordo, and T. Hrbek. 2015. Two new species of *Amazophrynella* (Amphibia: Anura: Bufonidae) from Loreto, Peru. *Zootaxa* 3946: 79–103.

Ron, S. R., W. E. Duellman, M. A. Caminer, and D. Pazmiño. 2018. Advertisement calls and DNA sequences reveal a new species of *Scinax* (Anura: Hylidae) on the Pacific lowlands of Ecuador. *PLoS ONE* 13: e0203169.

Ronquist, F., M. Teslenko, P. van der Mark, D. L. Ayres, A. Darling, S. Höhna, B. Larget, L. Liu, M. A. Suchard, and J. P. Huelsenbeck. 2011. MrBayes 3.2: efficient Bayesian phylogenetic inference and model choice across a large model space. *Systematic Biology* 61: 539–542.

Salducci, M. D., C. Marty, A. Fouquet, and A. Gilles. 2005. Phylogenetic relationships and biodiversity in hylids (Anura: Hylidae) from French Guiana. *Comptes Rendus Biologies* 328: 1009–1024.

Savage, J. M., and W. R. Heyer. 1967. Variation and distribution in the tree-frog genus *Phyllomedusa* in Costa Rica, Central America. *Beiträge zur Neotropischen Fauna* 5: 111–131.

Schulze, A., M. Jansen, and G. Köhler. 2015. Tadpole diversity of Bolivia's lowland anuran communities: molecular identification, morphological characterization, and ecological assignment. *Zootaxa* 4016: 1–111.

Spix, J. B. von. 1824. *Animalia nova sive Species novae Testudinum et Ranarum quas in itinere per Brasiliam annis MDCCCXVII–MDCCCXX jussu et auspiciis Maximiliani Josephi I. Bavariae Regis*. München, Germany: F. S. Hübschmann. [In Latin.]

Sturaro, M. J., and P. L. V. Peloso. 2014. A new species of *Scinax* Wagler, 1830 (Anura: Hylidae) from the middle Amazon River Basin, Brazil. *Papéis Avulsos de Zoologia* 54: 9–23.

Sueur, J., T. Aubin, and C. Simonis. 2008. Seewave, a free modular tool for sound analysis and synthesis. *Bioacoustics* 18: 213–226.

Tamura, K., G. Stecher, D. Peterson, A. Filipski, and S. Kumar. 2013. MEGA6: molecular evolutionary genetics analysis version 6.0. *Molecular Biology and Evolution* 30: 2725–2729.

Terra-Araujo, M. H., F. M. Costa, R. B. Carvalho, and A. Vicentini. 2015. *Ecclinusa campinae* (Sapotaceae), a new species from the Middle Rio Negro region, Amazonas, Brazil. *Brittonia* 67: 180–184.

Toledo, L. F., I. A. Martins, D. P. Bruschi, M. A. Passos, C. Alexandre, and C. F. B. Haddad. 2015. The anuran calling repertoire in the light of social context. *Acta Ethologica* 18: 87–99.

Trifinopoulos, J., L. T. Nguyen, A. von Haeseler, and B. Q. Minh. 2016. W-IQ-TREE: a fast online phylogenetic tool for maximum likelihood analysis. *Nucleic Acids Research* 44: 232–235.

Vacher, J. P., J. Chave, F. Ficetola, G. Sommeria-Klein, S. Tao, C. Thébaud, M. Blanc, A. Camacho, J. Cassimiro, T. J. Colston, M. Dewynter, R. Ernst, P. Gaucher, J. O. Gomes, R. Jairam, P. J. R. Kok, J. D. Lima, Q. Martinez, C. Marty, B. P. Noonam, P. M. S. Nunes, P. Ouboter, R. Recoder, M. T. Rodrigues, A. Snyder, S. Marques-Souza, and A. Fouquet. 2020. Large-scale DNA-based survey of frogs in Amazonia suggests a vast underestimation of species richness and endemism. *Journal of Biogeography* 47: 1781–1791.

Vicentini, A. 2016. The evolutionary history of *Pagamea* (Rubiaceae), a white-sand specialist lineage in tropical South America. *Biotropica* 48: 58–69.

von May, R., A. Catenazzi, R. Santa-Cruz, A. S. Gutierrez, C. Moritz, and D. L. Rabosky. 2019. Thermal physiological traits in tropical lowland amphibians: vulnerability to climate warming and cooling. *PLoS ONE* 14: e0219759.

Vriesendorp, C., N. Pitman, J. I. Rojas-Moscoso, B. A. Pawlak, L. Rivera-Chávez, L. Calixto-Méndez, M. Vela-Collantes, and E. P. Fasabi-Rimachi. 2006. Perú: Matsés. *The Field Museum, Rapid Biological Inventories Report 16*. Chicago: The Field Museum.

Wagler, J. 1830. *Natürliches System der Amphibien, mit vorangehender Classification der Säugthiere und Vogel. Ein Beitrag zur vergleichenden Zoologie*. München, Germany: Stuttgart and Tübingen: J. G. Cotta.

Wells, K. D. 1977. The social behaviour of anuran amphibians. *Animal Behaviour* 25: 666–693.